Bulletin of the Geological Society of Finland, Vol. 79, 2007, pp. 143–174

Intracratonic Palaeoproterozoic granitoids in northern Finland: prolonged and episodic crustal melting events revealed by Nd isotopes and U-Pb ages on zircon

Niina Ahtonen[1)]*, Pentti Hölttä[2)] and Hannu Huhma[2)]

[1)] *Geological Survey of Finland, P.O. Box 1237, FI-70211 Kuopio*

[2)] *Geological Survey of Finland, P.O. Box 96, FI-02151 Espoo*

Abstract

Zircons from twelve Palaeoproterozoic granitoids from the Central Lapland Granitoid Complex (CLGC) and from the Hetta Complex (HC) in northern Finland were dated using the NORDSIM ion microprobe. In addition, U-Pb age determinations on zircons from two samples were made using TIMS. Results reveal a wide range of U-Pb ages from 2.13 Ga to 1.76 Ga. The oldest samples include the porphyritic, weakly deformed Nilipää granite, which has an ion probe concordia age of 2126 ± 5 Ma, compatible with the previously published TIMS age of 2136 ± 5 Ma. The Tohmo granodiorite provided a slightly younger ion microprobe age of 2105 ± 4 Ma. The age of these two granitoids overlaps the depositional age of Karelian cratonic metasediments, suggesting that they represent an unusual tectonic setting for granitoid magmatism in the Fennoscandian Shield.

The Ruoppapalo granodiorite, which is also porphyritic and weakly deformed, yielded an ion probe zircon concordia age of 1905 ± 5 Ma, in accord with the conventional TIMS result. The strongly deformed Molkokõngäs granite has an ion probe concordia age of 1855 ±13 Ma, which is within error limits the same as the TIMS age, 1843 ± 23 Ma. The Pernu monzogranite has a concordia age of 1813 ± 6 Ma. All other granitoids in the CLGC, including those of appinitic affinity, as well as a leucosome from the Kappera migmatite in the Hetta Complex, are dated at 1.79 – 1.76 Ga, although many granitoids have older inherited zircons. The abundance of deformed granitoids of this age show that intensive ductile deformation, metamorphism and melting occurred at around 1.79 – 1.76 Ga in the northern Fennoscandian Shield, coeval with post-collisional magmatism in the southern part of the Shield.

Most granitoids in the Central Lapland Granitoid Complex have strongly negative ε_{Nd} values (1.8 Ga), ranging from -8 to -5. It is evident that they have a major Archaean component in their source, indicating derivation from Archaean crust during crustal reworking in an intracratonic tectonic setting.

Key words: granites, granodiorites, migmatites, Central Lapland Granitoid Complex, partial melting, absolute age, U/Pb, Sm/Nd, Paleoproterozoic, Lapland Province, Finland

*Corresponding author email: niina.ahtonen@gtk.fi

1. Introduction

Palaeoproterozoic granitoids cover large areas in Northern Fennoscandia, which records a prolonged Proterozoic tectonic history, commencing with rifting of the Archaean craton at around 2.5 – 2.4 Ga and culminating in collisional crustal thickening and orogenic collapse during the Lapland-Kola and the Svecofennian orogenies between 1.93 and 1.77 Ga (e.g. Meriläinen, 1976; Skiöld et al., 1993; Öhlander & Skiöld, 1994; Glebovitsky et al., 2001; Hanski et al., 2001a; Corfu & Evins, 2002; Lahtinen et al., 2005). The age determinations and geochemistry of the granitoids belonging to these orogenic events has been crucial in constraining timing and tectonic interpretations of orogenic events, crustal melting, deformation and pluton-related metamorphism (e.g. Hanski et al., 2001a; Lahtinen et al., 2005).

In this report we present Sm-Nd data on whole rock samples and ion microprobe and TIMS U-Pb data on zircons from granitoids and gneisses from the Central Lapland Granitoid Complex and from the Hetta Complex (Fig. 1). The sample set includes granitoids which had previously yielded TIMS ages that are unusual for Proterozoic granitoids in the Fennoscandian Shield and which therefore warranted further study by ion microprobe. In many cases these ages have also been difficult to interpret on the basis of structural field relations. The Nilipää granite, for example, is a very weakly deformed porphyritic rock with a zircon U-Pb TIMS age of 2.14 Ga (Huhma, 1986; Rastas et al., 2001). To our knowledge, this age is so far unique among granitoids in Fennoscandia. On the other hand, this age overlaps with the depositional age of rift-related volcanic rocks and sediments in Central Lapland (Hanski & Huhma, 2005 and references therein). The TIMS age of the very weakly deformed Ruoppapalo granodiorite, 1.92 Ga (Rastas et al., 2001) is also somewhat anomalous for Central Lapland, being significantly older than the main stages of granitoid magmatism, metamorphism and deformation which occurred in two main events, at around 1.88 Ga and 1.82 – 1.77 Ga (Hanski et al., 2001a; Lahtinen et al., 2005).

Apart from Nilipää and Ruoppapalo, our samples are from granitoids that are moderately or strongly deformed, and therefore expected to give the maximum age for deformation and metamorphism in those areas where the samples were taken. The deformed Molkokönġäs granite was selected for ion microprobe analysis because the existing TIMS zircon age of 1843 ± 23 Ma (Huhma, 1986) has relatively large error limits, and also because this age lies outside the main periods of granite magmatism. A further sample was taken from migmatite leucosome from the Hetta Complex, in an attempt to establish the timing of partial melting of the host rock, and hence the age of high grade metamorphism in the Hetta area. Several samples in our data set are from the eastern part of the Central Lapland Granitoid Complex where Proterozoic granitoids have so far been poorly dated. Samples were taken from around the Archaean Suomujärvi Complex where U-Pb ages on monazites and titanites show a strong metamorphic overprint at 1.78 – 1.77 Ga (Corfu & Evins, 2002), implying that surrounding granitoids might have formed during the same thermal event.

In addition to the dated specimens, a set of samples for Sm-Nd analyses was taken along a profile across the Central Lapland Granitoid Complex (Fig. 1). The negative ε_{Nd} values in most Palaeoproterozoic granitoids in Central Finnish Lapland (Huhma, 1986) as well as in the Lina granitoids in Northern Sweden (Öhlander & Skiöld, 1994) indicate that they were derived from melting of Archaean crust or sedimentary material of Archaean origin during Palaeoproterozoic orogenic processes. With our data set we intended to establish how valid this conclusion is for the Central Lapland Granitoid Complex in general.

2. Geological setting

The tectonic processes that have controlled the evolution of the geology of Central Finnish Lapland area (Fig. 1) are largely related to sequential rifting and tectonic thickening in an intracratonic environ-

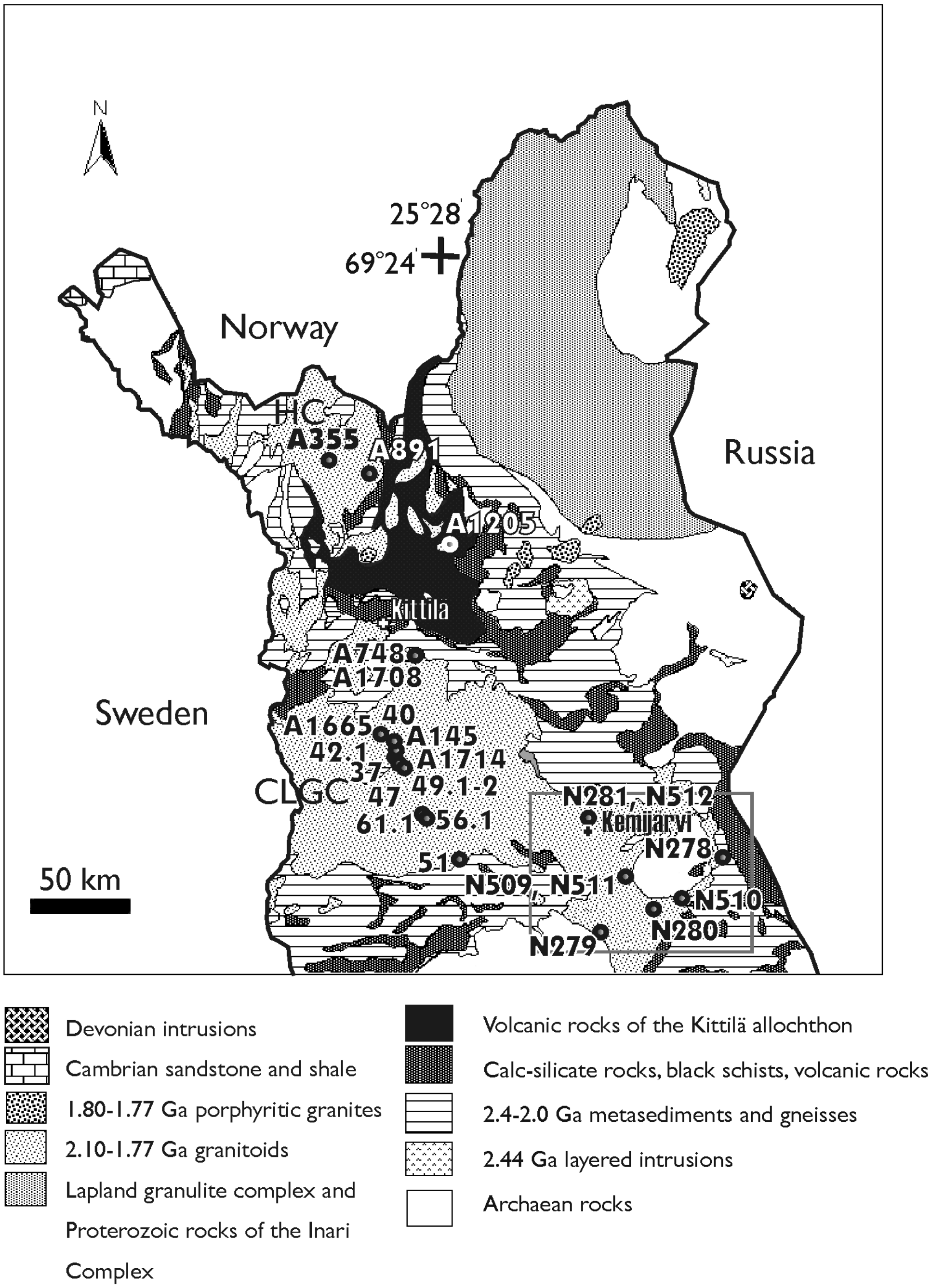

Fig. 1. Generalised geological map of the Finnish Lapland. Dots with numbers refer to the locations of the samples presented in Tables 2 and 3. HC = Hetta Complex, CLGC = Central Lapland Granitoid Complex. The grey box shows the location of Fig. 2.

ment, with the additional accretion of some allochthonous units (Hanski & Huhma, 2005). According to Hanski et al. (2001a), the Palaeoproterozoic evolution of the Central Lapland area commenced with rifting of the Archaean crust, producing felsic volcanic rocks of the Salla Group at around 2.43 – 2.48

Ga. These sub aerially erupted volcanic rocks were followed by crustally contaminated komatiites, siliceous high-Mg basalts and mafic volcanic rocks of the Onkamo Group. The 2.44 Ga Koitelainen layered intrusion intrudes the volcanic rocks of the Salla Group but not those of the Onkamo Group. This initial phase of rifting and volcanism was followed by deposition of arkosic quartzites, carbonate rocks and mica schists of the Sodankylä Group, some time before 2.2 Ga, when they were intruded by a distinctive suite of mafic/ultramafic sills known as the gabbro-wehrlite association (Hanski et al. 2001a; Hanski & Huhma, 2005 and references therein). The Sodankylä Group sedimentary rocks are also cut by 2.14 Ga old gabbro intrusions. The conventional U-Pb zircon age for the Nilipää granite is 2136 ± 5 Ma (Huhma, 1986; Rastas et al., 2001), which is thus coeval with these gabbros.

Deepening of the sedimentary basin caused accumulation of more fine-grained sediments represented by phyllites and black schists, belonging to the Savukoski Group. These pelitic metasediments are conformably overlain by basaltic and peridotitic komatiites and picrites, dated at 2.06 Ga using the Sm-Nd clinopyroxene-whole rock method (Hanski et al., 2001b). The 2.05 Ga Keivitsa mafic layered intrusion and several 2.05 Ga mafic dykes intruding the Savukoski Group provide minimum age constraints. The sedimentary-volcanic associations described above are in tectonic contact with the Kittilä Group, interpreted as an allochthonous oceanic unit comprising various MORB-, OIB- and IAT-type volcanic rocks, ophiolitic mantle rocks of the Nuttio Complex, and chemical sediments (Hanski, 1997; Hanski & Huhma, 2005). Felsic porphyries, which are demonstrably coeval with the mafic volcanic rocks of the Kittilä Group, have been dated at 2.01 Ga. The Ruoppapalo porphyritic granodiorite in the northern part of the Kittilä Group has a zircon U-Pb age of 1914 ± 3 Ma (Huhma, 1986; Rastas et al., 2001). The Nyssäkoski felsic dyke, which is discordant across Kittilä Group rocks has an age of 1919 ± 8 Ma, and is also geochemically similar to the Ruoppapalo granodiorite (Rastas et al., 2001; Hanski & Huhma, 2005). Younger quartzites and conglomerates of the Lainio and the Kumpu Groups lie unconformably on the above mentioned rock units. These molasse-type sediments contain pebbles of ca. 1.88 Ga magmatic rocks, which thus define a maximum age for sedimentation (Hanski et al., 2000).

The bedrock in the northern part of the Central Lapland area was reworked by the Lapland-Kola orogen at 1.93 – 1.91 Ga, when the Kola Craton collided with the Karelian Craton (Berthelsen & Marker, 1986; Daly et al., 2001, Lahtinen et al., 2005). From 1.91 Ga to 1.77 Ga the Central Lapland area was affected by granitoid magmatism, greenschist to amphibolite facies metamorphism and compressional deformation that produced e.g. fold and thrust belt with nappes (Koistinen, 1981; Ward et al., 1989; Tuisku & Huhma, 1998; Lehtonen et al., 1998; Evins & Laajoki, 2002; Hölttä et al., 2007). Svecofennian granitoids are widespread especially in western Finnish Lapland, where they are assigned to the Haaparanta (Haparanda) Suite. Numerous zircon age determinations have been made for Haaparanta Suite rocks, ranging from 1890 to1860 Ma (Hiltunen, 1982, Väänänen & Lehtonen, 2001; Hanski et al., 2001a). Granitoids of this age are uncommon in eastern Lapland, but Räsänen & Huhma (2001) reported an age of 1891 ± 5 Ma for granodiorite from Kelujärvi, east of the Sodankylä Township. The Tepasto and Kihlanki granites in western Finnish Lapland are dated at 1802 ± 10 and 1805 ± 15 Ma, respectively (Rastas et al., 2001; Väänänen & Lehtonen, 2001). The Nattanen granites form a group of plutons transecting the southern margin of the Lapland Granulite Complex and have been dated at 1.79 – 1.77 Ga (Huhma, 1986). Near the southern margin of the Central Lapland Granitoid Complex, at the Rovaniemi airport, the Maununmatti porphyritic granite gives an age of 1770 ± 8 Ma (Lauerma, 1982).

3. Samples

3.1. Western Lapland

The *Molkoköngäs granite* (A145) is pink and coarse grained, with a prominent foliation and lineation attributed to regional D2 or D3 deformation, so that the age determination for this rock should also give the maximum age for the foliation in this locality. The slightly heterogeneous conventional U-Pb data on zircon have yielded an upper intercept age of 1843 ± 23 Ma (MSWD=10), while an initial ε_{Nd}(1.84 Ga) of -6.9 ± 0.7 was calculated from the whole rock Sm-Nd analysis (Huhma, 1986). As the error limits are high and rocks of this age are rare in Lapland, it was expected that the rock might contain a mixed population of zircons of various ages.

The *Nilipää granite* (A748), at the northern edge of the Central Lapland Granitoid Complex (Fig. 1) is porphyritic, coarse grainedand weakly deformed. The country rock is metasedimentary mica gneiss, interpreted to belong to the Sodankylä Group. The metamorphic grade of the country rocks increases from andalusite to sillimanite grade towards the contacts of the Nilipää granite, suggestive of a thermal aureole surrounding the intrusion (Hölttä et al., 2007). The TIMS U-Pb discordia age on zircons is 2136 ± 5Ma (MSWD=0.002) and the ε_{Nd}(2.14 Ga) is -2.5 ± 0.5 (Huhma, 1986; Rastas et al., 2001). An additional sample (A1708) was taken from the Iso Nilipää site in order to confirm the previous sampling (map coordinates 7493483/2555139).

The *Kappera sample* (A891) is from a tonalitic leucosome of a migmatitic grey biotite gneiss. It has a heterogeneous zircon population, while the U-Pb age of titanite is 1.77 Ga (Mänttäri, 1995). The rock has a flat-lying pervasive foliation, which is very typical of both granitoids and supracrustal rocks in extensive areas south and southwest of the Lapland granulite belt. We therefore expected to get the age of melting and high-grade metamorphism as well as the maximum age of deformation by dating the leucosome in this migmatite.

The *Ruoppapalo granodiorite* (A1206) is porphyritic, coarse grained and weakly deformed. It is in-

Table 1. Chemical compositions of the Jääskö monzonite. The analyses have been made at the Geolaboratory of the Geoservice Center, Geological Survey of Finland. The REEs were analysed using the ICP-MS and other elements using the XRF method.

Sample	PSH-01-45.1	PSH-01-45.2	PSH-01-45.5
SiO_2 (wt.%)	53.88	50.45	55.24
TiO_2	2.03	2.38	1.72
Al_2O_3	16.01	15.73	15.30
FeO	10.01	11.92	8.89
MnO	3.28	4.28	4.26
MgO	0.11	0.15	0.13
CaO	5.80	7.00	5.13
Na_2O	4.33	4.65	4.19
K_2O	2.68	1.68	2.38
P_2O_5	1.04	1.01	0.86
Ba (ppm)	2047	1227	1770
Cl	953	644	1012
Cr	29	53	115
Cu	19	52	41
Ga	25	32	26
Nb	22	20	16
Ni	13	28	31
Rb	69	39	69
S	1874	2994	596
Sr	1031	883	945
V	178	210	143
Zn	120	133	127
Zr	405	224	196
Ce	209	146	162
Dy	4.77	5.36	3.99
Er	1.97	2.21	1.79
Eu	2.78	3.01	2.56
Gd	9.25	9.62	7.74
Ho	0.78	0.93	0.73
La	108	68.7	82.8
Lu	0.21	0.23	0.22
Nd	86.1	66.0	65.3
Pr	22.2	16.6	18.2
Sc	17.2	21.4	15.9
Sm	11.8	10.8	10.4
Tb	1.15	1.14	0.94
Th	3.05	2.87	5.04
Tm	0.26	0.30	0.25
U	0.55	0.67	1.14
Y	23.6	26.4	20.3
Yb	1.53	1.79	1.55
F	0.25	0.21	0.17
C	0.04	0.07	0.04

trusive into Kittilä Group mafic metavolcanic rocks which have yielded ages of 1.99 – 2.02 Ga (Hanski & Huhma, 2005). The conventional zircon age is 1914 ± 3 Ma (MSWD=0.12, n=3; Rastas et al., 2001) and Hanski & Huhma (2005) calculated a value for ε_{Nd}(1.91 Ga) of -1.5. Because the Ruoppapalo intrusion cuts the Kittilä Group rocks, its age has been considered as the minimum time for the emplacement of the Kittilä allochthon (Hanski et al., 2001a).

The *Jääskö monzonite* (A1714) is situated along the river Ounasjoki, ca. 4 km south of Molkokönġäs. The most common rock type in the area is coarse-grained granite, whereas the Jääskö monzonite represents a less abundant rock type that seems to cut the granites. The Jääskö monzonite belongs to the appinitic series of intrusions which have bee found in several places in the Central Lapland Granitoid Complex (Mutanen, 2003; Mutanen & Väänänen, 2004). Chemical composition of the Jääskö monzonite is presented in Table 1. In outcrop the monzonite contains gabbroic and amphibolitic enclaves and is cut by granite dikes.

The *Tainio gabbro*, located close to the Jääskö monzonite, also belongs to the appinite series, with a zircon U-Pb age of 1796 ± 4 Ma (Väänänen, 2004). Appinites are normally weakly deformed or undeformed, having high alkali abundances and high LREE, Ba, Sr, Ni, Cr, Zr, P, Cl and F. They resemble post-collisional shoshonitic rocks of the southern Svecofennian belt, although there are also some significant differences, such as lower REE and K_2O in the Lapland appinites (Eklund et al., 1998; Eklund, 2006; Mutanen, 2003; Andersson et al., 2006; Eklund, pers. comm., 2006; Mutanen, pers. comm., 2006). According to the classification of de la Roche et al. (1980) the analysed samples (Table 1) are monzonites and syenodiorites.

3.2. Eastern Lapland

Figure 2 shows the location of the samples taken from around the Archaean Suomujärvi Complex on an airborne magnetic map. Because this area is poorly exposed and mapped, the field relationships of the various rock types are difficult to establish. No previous isotopic data are available for these granitoids.

The *Palotunturi granite* (N278) in the eastern part of the Central Lapland Granitoid Complex forms a roundish, weakly magnetic stock, which is discordant with respect to country rock structures. The granites of Palotunturi area are medium grained, light grey to dark red in colour and deformed (Airo & Ahtonen, 1999). The Pernu area consists of heterogeneous granitoids apparently lacking sharp contacts with enclosing Archaean gneisses (Airo & Ahtonen, 1999). Sample N279 represents the most abundant granite type, which is medium-grained, deformed and reddish in colour. The bedrock of the Pernu area has previously been interpreted as part of the Archaean basement complex (Korsman et al., 1997).

The *Jumisko granitoids* form narrow elongated NW-SE trending bodies between the Pernu area and the Archaean Suomujärvi Complex (Airo & Ahtonen, 1999; Evins et al., 2002). The Jumisko monzogranite (N280) is a medium to coarse-grained, slightly deformed homogenous rock. Sample N281 is from a quarry in Tohmo, north of Kemijärvi, and represents strongly deformed medium grained granodiorite. Sample N512 is also from the Tohmo quarry, from a deformed red monzogranite dyke discordant across the granodiorite. The Petäjäselkä granodiorite is located NW of the Jumisko area, sample N509 being from a medium to coarse-grained, hornblende bearing and deformed granodiorite. The Petäjäselkä monzogranite (N511) is a coarse-grained, K-feldspar porphyric pink foliated rock. The monzogranite has many biotite-rich gneiss inclusions which locally comprise > 50 % of the rock, forming a stromatic migmatite, so that the monzogranite can be considered as a leucosome. The Vääräjärventie granite N510 is from a strongly deformed, medium grained magnetite-bearing granite.

4. Analytical methods

4.1. Sm-Nd method

Sm-Nd analyses were done at the Isotope Geological Laboratory of the Geological Survey of Finland.

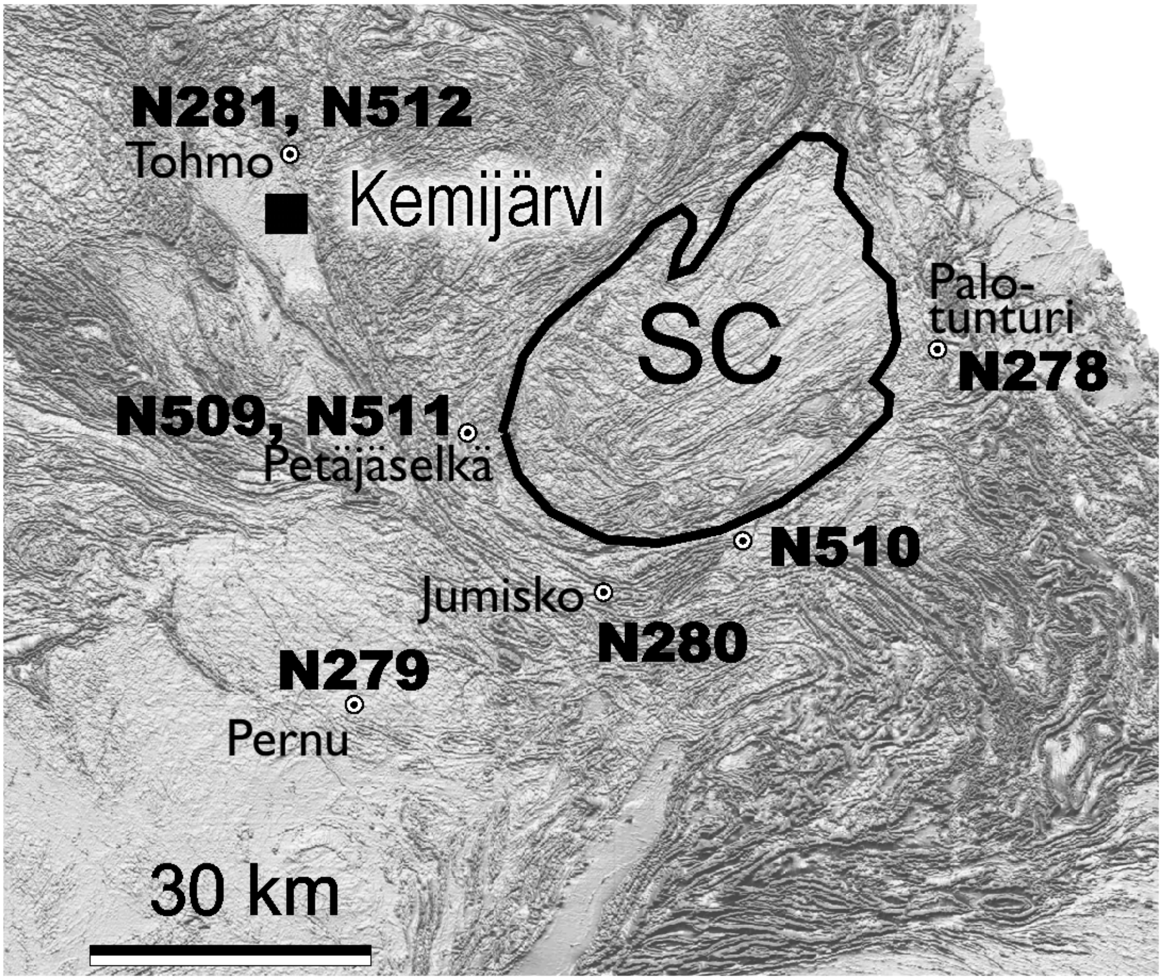

Fig. 2. An airborne magnetic map showing the locations of the Archaean Suomujärvi Complex (SC) and the samples of the eastern Lapland in this study.

The whole rock powder (150 mg) was dissolved for 48h in HF-HNO_3 using sealed teflon bombs. Mixed ^{149}Sm-^{150}Nd spike was added to the sample prior the dissolution. After careful evaporation of fluorides the residue was dissolved in 6N HCl and a clear solution was achieved. Sm and Nd were separated in two stages using a conventional cation-exchange procedure (7 ml of AG50Wx8 ion exchange resin in a bed of 12 cm length) and a modified version of the Teflon-HDEHP (hydrogen di-ethylhexyl phosphate) method developed by Richard et al. (1976). The measurements have been made in a dynamic mode on a VG SECTOR 54 mass-spectrometer using Ta-Re triple filaments. ^{143}Nd/^{144}Nd ratio is normalised to ^{146}Nd/^{144}Nd=0.7219. The average value for La Jolla standard is ^{143}Nd/^{144}Nd = 0.511850 ± 10 (std, n=50, during 2002 – 2004). The Sm/Nd ratio of the spike was calibrated against the Caltech mixed Sm/Nd standard (Wasserburg et al, 1981). Based on duplicated analyses the error in ^{147}Sm/^{144}Nd is estimated to be 0.4 %. Initial ^{143}Nd/^{144}Nd and ε were calculated with the following parameters: λ^{147}Sm=6.54x10^{-12}a^{-1}, ^{147}Sm/^{144}Nd=0.1966 and ^{143}Nd/^{144}Nd=0.51264 for present CHUR. The depleted mantle model ages (T_{DM}) were calculated according to DePaolo (1981). Measurement on the rock standard BCR-1 provided the following values: Sm=6.58 ppm, Nd=28.8 ppm ^{147}Sm/^{144}Nd=0.1380, ^{143}Nd/^{144}Nd=0.51264 ±

0.00002. The blank measured during analyses was: 30 – 100 pg for Sm and 100 – 300 pg for Nd. The Isoplot software by Ludwig (2001) has been used for age calculations and data plotting.

4.2. Ion microprobe U-Pb dating

The ion microprobe analyses were performed using the Cameca IMS 1270 electron microprobe at the Swedish Museum of Natural History, Stockholm (NORDSIM facility). The spot diameter for the 4nA primary O^{2}- ion beam was ca. 30 μm and oxygen flooding in the sample chamber was used to increase the production of Pb+ ions. Four counting blocks comprising a total of twelve cycles of the Pb, Th and U species were measured in each spot. The mass resolution (M/ΔM) was 5400 (10 %). The raw data was calibrated against a zircon standard (91500; Wiedenbeck et al., 1995) and corrected for background at mass 204.2 and modern common lead (T=0; Stacey & Kramers, 1975). For further details of the analytical procedures see Whitehouse et al. (1997, 1999). The age calculations were done using the Isoplot/Ex program (Ludwig, 2001).

4.3. TIMS U-Pb dating

The TIMS age determination was done at the Isotope Geological Laboratory of the Geological Survey of Finland. The decomposition of zircons and extraction of U and Pb for conventional isotopic age determinations followed mainly the procedure described by Krogh (1973). ^{235}U-^{208}Pb-spiked and non-spiked isotopic ratios were measured using a VG Sector 54 thermal ionisation multicollector mass spectrometer. The measured U and Pb isotopic ratios were normalised according to the accepted ratios of SRM 981 and U500 standards. The U-Pb age calculations were done using the PbDat-program (Ludwig, 1991) and the fitting of the discordia line using the Isoplot/Ex program (Ludwig, 2001).

5. Results

A145 Molkokongäs granite (N996)

In the Molkokongäs sample, the zircon grains in the 4.55 – 4.44 gcm^{-3} density fraction are mainly fine-grained (-200 mesh), almost colourless and elongated. Many of the zircons are fragmented. Among these, a few very large brownish grains occur. In the lighter density fraction (4.3 – 4.2 gcm^{-3}), the mainly prismatic and brownish or colourless zircons were sieved into two grain-size fractions (-200 mesh and 100 – 200 mesh). Some zircons are reddish due to iron pigmentation. Among these there were a few fragments of larger, extremely transparent grains with slightly reddish tint, resembling metamorphic zircon. In backscattered electrons (BSE) images the internal zircon structures show mostly sector-zoned interiors with darker alteration material concentrated in certain zones. Many of these grains have narrow, distinct rims (Fig. 3a). A few zircons show smooth vague zoning, possibly because of partial destruction of previously sharp zoning.

Four of the ten analysed zircon domains provide discordant data and two of these show quite low $^{206}Pb/^{204}Pb$ ratios (Table 2). The analysis n996-02a from the rim is extremely discordant, while the zoned interior of the same zircon gives a concordant $^{207}Pb/^{206}Pb$ age of 1846 ± 22 Ma. Nine of the ten analysed zircon domains plot on a discordia line with an upper intercept age of 1845 ± 13 Ma (MSWD=3.5; n=9). The concordia age for the four concordant data points is 1855 ± 13 Ma (Fig. 4a). These ages are equal within the error limits, and they do not deviate from the TIMS age published previously by Huhma (1986). One analysis from an internally structureless zircon gives a concordant age of ca. 1.80 Ga. This may represent a healing effect due to later metamorphism.

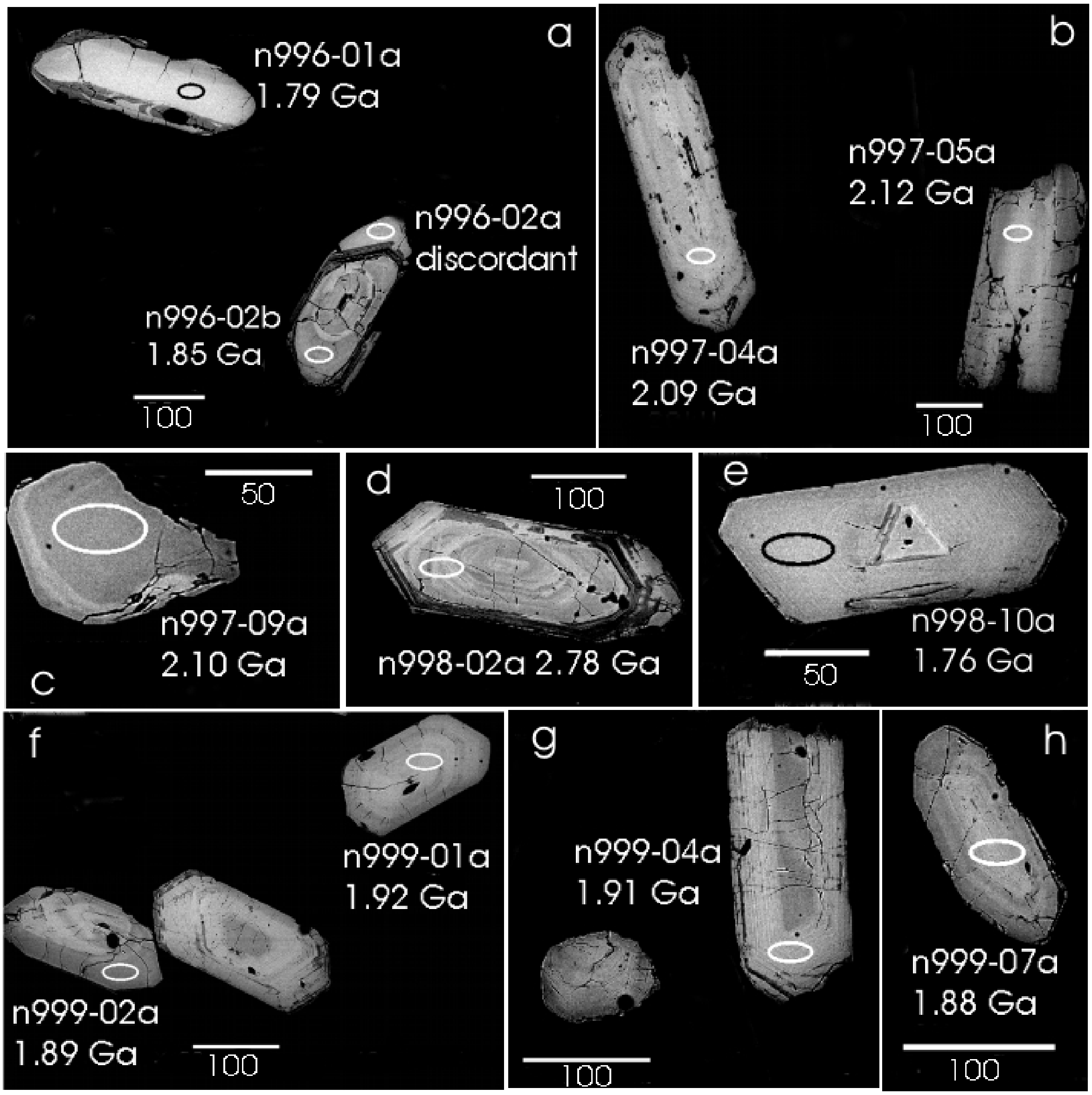

Fig. 3. BSE images of zircons. The number at the scale bar refers to microns.

A1714 Jääskö monzonite, TIMS U-Pb dating

Mineral separation of sample A1714 yielded abundant zircon, which occurs as light-coloured, clear, euhedral simple prisms. The four conventional analyses show relatively low concentrations of U in zircon, and provide nearly equal data close to the concordia-curve (Table 3, Fig. 5). An age of 1796 ± 3 Ma can be calculated assuming a lower intercept of 300 ± 300 Ma, which should cover all conceivable estimates. This age is equal with the U-Pb zircon age obtained recently from the Tainio gabbro (A1665; Väänänen, 2004), which is located ca. ten kilometres north of Jääskö. These rocks also provide equal initial ε_{Nd} of -5 (Table 4), and are likely members of the same rock association.

Table 2. Ion microprobe U-Pb data

		derived ages						corrected ratios								elemental data			
Sample/ spot	Zircon zoning and morphology*	$^{207}Pb/^{206}Pb$	±σ	$^{207}Pb/^{235}U$	±σ	$^{206}Pb/^{238}U$	±σ	$^{207}Pb/^{206}Pb$	±σ %	$^{207}Pb/^{235}U$	±σ %	$^{206}Pb/^{238}U$	±σ %	r	Disc.% 2σ lim.	U ppm	Th ppm	Pb ppm	$^{206}Pb/^{204}Pb$ measured
A145 Molkokongäs granite																			
n996-01a	unzoned, euhedral	1791	9	1810	15	1827	27	0.1095	0.47	4.948	1.74	0.3277	1.67	0.96		570	521	254	29561
n996-02a	unzoned edge	1776	9	1464	14	1259	19	0.1086	0.49	3.230	1.74	0.2157	1.67	0.96	-28.8	867	349	225	4011
n996-02b	zoned, euhedral	1846	11	1875	15	1902	28	0.1129	0.61	5.340	1.78	0.3431	1.68	0.94		214	199	100	14963
n996-03a	unzoned, euhedral	1853	8	1863	15	1872	28	0.1133	0.44	5.262	1.76	0.3369	1.70	0.97		565	438	253	5327
n996-04a	weakly zoned, euhedral	1840	26	1729	19	1639	25	0.1125	1.42	4.489	2.24	0.2894	1.72	0.77	-5.2	246	174	93	453
n996-05a	unzoned, euhedral	1834	7	1834	15	1835	27	0.1121	0.37	5.090	1.71	0.3294	1.67	0.98		1131	1526	541	39646
n996-06a	weakly zoned, long prism	1866	4	1847	15	1830	28	0.1141	0.24	5.166	1.78	0.3284	1.76	0.99		812	704	358	9270
n996-07a	weakly zoned, long prism	1823	8	1795	15	1771	27	0.1115	0.45	4.858	1.82	0.3161	1.76	0.97		478	392	203	6190
n996-08a	weakly zoned, euhedral	1837	13	1773	16	1720	27	0.1123	0.75	4.733	1.93	0.3057	1.78	0.92	-2.5	279	200	113	588
n996-09a	weakly zoned, oval	1819	13	1755	16	1701	26	0.1112	0.70	4.631	1.90	0.3020	1.76	0.93	-2.8	244	224	102	9186
A748 Nilipää granite																			
n997-01	weakly zoned, euhedral	2135	8	2132	15	2129	30	0.13279	0.43	7.1646	1.70	0.39130	1.65	0.97		278	140	138	22890
n997-02	weakly zoned, euhedral	2122	4	2134	15	2147	30	0.13180	0.21	7.1824	1.68	0.39522	1.66	0.99		1007	429	498	29030
n997-03	weakly zoned, euhedral	2132	4	2136	15	2140	31	0.13252	0.24	7.1922	1.70	0.39363	1.68	0.99		1007	604	516	22409
n997-04	weakly zoned, euhedral	2091	5	2115	16	2140	31	0.12952	0.31	7.0318	1.74	0.39375	1.72	0.98		1035	691	532	2469
n997-05	weakly zoned, euhedral	2119	6	2149	15	2179	31	0.13160	0.34	7.2988	1.69	0.40227	1.66	0.98		367	485	223	29111
n997-06	weakly zoned, euhedral, edge	2121	4	2149	15	2179	32	0.13169	0.21	7.3017	1.72	0.40212	1.71	0.99		1398	750	719	82520
n997-07a	weakly zoned, euhedral	2122	7	2101	16	2079	32	0.13181	0.40	6.9180	1.82	0.38066	1.78	0.98		352	469	202	10245
n997-08a	unzoned, euhedral	2134	4	2106	17	2077	34	0.13273	0.25	6.9591	1.91	0.38026	1.89	0.99		796	270	372	62876
n997-09a	unzoned, short prism	2099	21	2094	20	2089	33	0.13011	1.23	6.8659	2.22	0.38273	1.84	0.83		34	38	19	6550
n997-10a	weakly zoned, oval	2105	5	2099	16	2094	32	0.13053	0.29	6.9064	1.79	0.38375	1.77	0.99		614	505	321	10250

Table 2. cont. Ion microprobe U-Pb data

Sample/ spot	Zircon zoning and morphology*	derived ages $^{207}Pb/^{206}Pb$	±σ	$^{207}Pb/^{235}U$	±σ	$^{206}Pb/^{238}U$	±σ	corrected ratios $^{207}Pb/^{206}Pb$	±σ %	$^{207}Pb/^{235}U$	±σ %	$^{206}Pb/^{238}U$	±σ %	r	Disc.% 2σ lim.	elemental data U ppm	Th ppm	Pb ppm	$^{206}Pb/^{204}Pb$ measured
A891 Kappera migmatite																			
n998-01a	unzoned, euhedral	2390	4	2326	15	2254	32	0.1539	0.23	8.881	1.67	0.4185	1.65	0.99	-3.5	1613	143	795	124655
n998-02a	weakly zoned, euhedral	2781	5	2785	17	2790	40	0.1945	0.31	14.524	1.78	0.5416	1.75	0.98		282	128	201	47301
n998-03a	unzoned, euhedral	1801	16	1791	16	1783	27	0.1101	0.86	4.837	1.91	0.3187	1.70	0.89		1994	1770	865	212973
n998-04a	unzoned, euhedral	1777	3	1802	14	1825	27	0.1086	0.16	4.900	1.69	0.3272	1.68	1.00		2060	1048	842	131941
n998-05a	zoned, long prism	1736	10	1682	11	1639	17	0.1063	0.56	4.242	1.33	0.2895	1.20	0.91	-2.8	230	129	85	4911
n998-06a	zoned, long prism	1769	5	1751	23	1736	41	0.1082	0.28	4.610	2.72	0.3091	2.70	0.99		896	757	366	21605
n998-07a	zoned, long prism	1073	36	1067	22	1064	27	0.0752	1.84	1.859	3.27	0.1794	2.71	0.83		106	41	22	6653
n998-08a	zoned, short prism	1769	4	1798	24	1823	44	0.1082	0.21	4.874	2.76	0.3268	2.75	1.00		1939	2248	890	24302
n998-09a	zoned, euhedral	1782	5	1804	24	1823	44	0.1089	0.30	4.907	2.76	0.3267	2.74	0.99		1208	478	485	17967
n998-10a	zoned, euhedral	1764	5	1789	23	1811	43	0.1079	0.30	4.824	2.74	0.3243	2.72	0.99		1612	1806	731	44395
A1206 Ruoppapalo granodiorite																			
n999-01a	zoned, euhedral	1921	4	1958	11	1994	21	0.1177	0.24	5.881	1.23	0.3625	1.20	0.98	1.6	1332	490	589	65555
n999-02a	unzoned rim, metam.?	1894	12	1913	12	1932	20	0.1159	0.67	5.582	1.37	0.3494	1.19	0.87		240	43	98	26684
n999-03a	unzoned, euhedral	1902	7	1943	13	1982	24	0.1164	0.41	5.781	1.46	0.3600	1.41	0.96	1.4	1293	369	558	35742
n999-04a	zoned, euhedral	1909	5	1926	24	1942	46	0.1169	0.28	5.666	2.75	0.3516	2.73	0.99		1168	200	478	28341
n999-05a	unzoned, oval	1911	13	1836	24	1770	42	0.1170	0.72	5.099	2.82	0.3160	2.73	0.97	-2.5	848	299	323	1715
n999-06a	zoned, euhedral	1917	9	1868	24	1825	43	0.1174	0.51	5.297	2.76	0.3273	2.71	0.98		1334	286	513	10193
n999-07a	zoned, euhedral	1878	10	1929	25	1977	47	0.11489	0.57	5.6862	2.83	0.35896	2.77	0.98		945	293	404	4280
n999-10a	zoned, oval	1911	4	1890	24	1871	44	0.1170	0.25	5.432	2.72	0.3368	2.70	1.00		815	187	324	29715
n999-11a	weakly zoned, euhedral	1907	7	1873	24	1843	45	0.1168	0.39	5.327	2.81	0.3309	2.79	0.99		693	197	274	5156
n999-12a	zoned, oval	1900	6	1921	16	1941	30	0.1163	0.32	5.634	1.83	0.3514	1.80	0.98		612	120	252	21736
n999-13a	weakly zoned, euhedral	1906	4	1897	16	1889	29	0.1167	0.22	5.480	1.80	0.3405	1.79	0.99		794	234	326	11780
n999-14a	weakly zoned, euhedral	1900	5	1882	16	1865	29	0.1163	0.26	5.382	1.82	0.3356	1.80	0.99		650	144	258	30688

Table 2. cont. Ion microprobe U-Pb data

Sample/ spot	Zircon zoning and morphology*	derived ages $^{207}Pb/^{206}Pb$	±σ	$^{207}Pb/^{235}U$	±σ	$^{206}Pb/^{238}U$	±σ	corrected ratios $^{207}Pb/^{206}Pb$	±σ %	$^{207}Pb/^{235}U$	±σ %	$^{206}Pb/^{238}U$	±σ %	r	Disc.% 2σ lim.	elemental data U ppm	Th ppm	Pb ppm	$^{206}Pb/^{204}Pb$ measured
N278 Palotunturi granite																			
n278-01a	weakly zoned, euhedral	1757	7	1808	19	1852	35	0.10749	0.41	4.9329	2.23	0.33283	2.19	0.98	1.2	231	137	98	16912
n278-04a	unzoned core, oval	1950	4	2011	19	2070	38	0.11957	0.20	6.2439	2.14	0.37872	2.13	1.00	2.6	2251	1782	1148	4151
n278-04b	weakly zoned rim	1963	7	1953	19	1944	36	0.12048	0.38	5.8470	2.19	0.35199	2.15	0.99		467	311	214	1667
n278-05a	unzoned core, oval	1928	8	1960	20	1991	38	0.11810	0.44	5.8941	2.24	0.36197	2.20	0.98		173	115	82	244021
n278-06a	zoned, oval	1774	7	1798	19	1820	34	0.10848	0.37	4.8778	2.20	0.32612	2.17	0.99		363	216	152	3382
n278-19a	weakly zoned, euhedral	1767	5	1783	18	1796	34	0.10808	0.27	4.7891	2.17	0.32136	2.15	0.99		445	259	183	32595
n278-20a	unzoned, rounded	2717	6	2768	22	2837	52	0.18715	0.38	14.2682	2.29	0.55295	2.25	0.99	0.5	102	53	76	16124
n278-20b	unzoned edge	1761	3	1827	18	1886	35	0.10768	0.16	5.0473	2.14	0.33995	2.13	1.00	3.6	1543	550	636	21978
n278-24a	zoned, oval	2687	6	2693	22	2701	51	0.18380	0.34	13.1859	2.32	0.52031	2.29	0.99		169	153	125	90090
n278-24b	unzoned edge	2025	11	1989	20	1953	38	0.12475	0.62	6.0881	2.31	0.35394	2.23	0.96		646	279	287	90253
n278-26a	weakly zoned, euhedral	1749	9	1777	19	1801	34	0.10703	0.47	4.7557	2.21	0.32226	2.16	0.98		350	306	155	1849
n278-29a	weakly zoned, oval	1977	3	2001	19	2023	37	0.12141	0.16	6.1721	2.14	0.36871	2.13	1.00		1464	810	691	142410
n278-37a	unzoned, euhedral	1960	12	1899	19	1843	34	0.12026	0.69	5.4873	2.24	0.33092	2.13	0.95	-1.9	1250	885	545	482
n278-48a	weakly zoned, euhedral	1748	7	1780	19	1807	35	0.10697	0.38	4.7726	2.24	0.32360	2.20	0.99		237	133	97	25595
N279 Pernu monzogranite																			
n279-04a	unzoned edge, euhedral	1781	19	1768	20	1757	33	0.10892	1.06	4.7067	2.39	0.31341	2.13	0.90		3753	1978	1479	2623
n279-07a	weakly zoned, euhedral	1819	7	1819	19	1819	35	0.11120	0.39	4.9980	2.23	0.32598	2.20	0.98		171	33	65	92764
n279-08a	unzoned edge, euhedral	2853	3	2861	21	2872	51	0.20329	0.21	15.7325	2.18	0.56127	2.17	1.00		548	60	379	38715
n279-11a	weakly zoned, euhedral	1809	6	1829	19	1846	35	0.11060	0.32	5.0567	2.18	0.33160	2.16	0.99		432	134	171	190549
n279-26a	weakly zoned, short prism	1819	10	1844	20	1866	36	0.11120	0.58	5.1479	2.28	0.33575	2.21	0.97		161	43	64	165453
n279-30a	weakly zoned, oval	2470	18	2468	23	2466	46	0.16140	1.06	10.3687	2.47	0.46593	2.23	0.90		121	123	82	105764
n279-35a	weakly zoned, oval	1806	7	1807	19	1807	35	0.11040	0.37	4.9249	2.26	0.32354	2.23	0.99		225	68	87	>1e6
n279-41a	weakly zoned core of rounded zr	2000	193	835	70	468	10	0.12297	11.61	1.2760	11.80	0.07525	2.13	0.18	-22.9	58	17	8	42
n279-45a	unzoned core of rounded zr	1813	6	1814	19	1816	35	0.11080	0.35	4.9695	2.23	0.32529	2.21	0.99		228	84	90	71736
n279-45b	unzoned edge	1601	66	1260	31	1070	21	0.09876	3.63	2.4577	4.21	0.18048	2.12	0.51	-17.8	2602	1669	548	279
n279-48a	weakly zoned core of euhedral zr	2934	8	2927	22	2917	52	0.21370	0.52	16.8581	2.27	0.57214	2.21	0.97		179	65	134	127146
n279-60a	weakly zoned, euhedral	1813	8	1813	19	1814	35	0.11083	0.42	4.9652	2.22	0.32493	2.19	0.98		561	164	217	4021

Table 2. cont. Ion microprobe U-Pb data

Sample/ spot	Zircon zoning and morphology*	derived ages $^{207}Pb/^{206}Pb$	±σ	$^{207}Pb/^{235}U$	±σ	$^{206}Pb/^{238}U$	±σ	corrected ratios $^{207}Pb/^{206}Pb$	±σ %	$^{207}Pb/^{235}U$	±σ %	$^{206}Pb/^{238}U$	±σ %	r	Disc.% 2σ lim.	elemental data U ppm	Th ppm	Pb ppm	$^{206}Pb/^{204}Pb$ measured
N280 Jumisko monzogranite																			
n280-09a	zoned, oval	1751	6	1802	18	1847	35	0.10710	0.31	4.8995	2.17	0.33179	2.15	0.99	1.5	728	980	359	150128
n280-11a	zoned, oval	1766	6	1775	19	1783	35	0.10800	0.33	4.7431	2.24	0.31852	2.21	0.99		508	321	209	131527
n280-12a	zoned, oval	1762	3	1784	18	1803	34	0.10774	0.16	4.7928	2.15	0.32263	2.14	1.00		1333	392	509	52549
n280-13a	zoned, oval	1761	4	1793	18	1821	34	0.10772	0.22	4.8467	2.14	0.32633	2.13	0.99		840	181	321	35562
n280-23a	weakly zoned core of oval zr	2536	5	2484	21	2421	45	0.16780	0.31	10.5432	2.27	0.45570	2.25	0.99	-1.0	170	131	105	147232
n280-24a	weakly zoned, euhedral	1724	17	1552	19	1429	28	0.10554	0.91	3.6103	2.40	0.24810	2.21	0.92	-13.5	180	234	59	791
n280-25a	unzoned, oval	1751	8	1735	19	1721	33	0.10712	0.44	4.5196	2.23	0.30601	2.18	0.98		615	237	222	4151
n280-28a	weakly zoned, oval	1760	4	1785	18	1807	34	0.10766	0.22	4.8026	2.16	0.32353	2.15	0.99		993	1321	482	6676
n280-42a	zoned, euhedral	1763	3	1830	19	1890	36	0.10781	0.14	5.0638	2.20	0.34066	2.19	1.00	3.5	1538	218	601	148633
N281 Tohmo granodiorite																			
n281-03a	weakly zoned, euhedral	2100	5	2091	22	2081	44	0.13018	0.29	6.8396	2.49	0.38104	2.47	0.99		1017	405	480	4102
n281-04a	weakly zoned, euhedral	2107	3	2146	20	2187	42	0.13070	0.15	7.2807	2.24	0.40401	2.24	1.00		1048	1281	625	309119
n281-08a	weakly zoned, euhedral	2108	4	2129	20	2152	41	0.13072	0.25	7.1416	2.24	0.39625	2.22	0.99		360	7	162	46382
n281-18a	weakly zoned, euhedral	2100	3	2106	19	2113	39	0.13013	0.16	6.9588	2.14	0.38786	2.13	1.00		1302	646	641	75415
n281-19a	weakly zoned, euhedral	2108	4	2160	20	2214	40	0.13076	0.21	7.3896	2.16	0.40987	2.15	1.00	1.3	3721	1269	1873	14004
n281-24a	zoned long prism	2104	4	2153	19	2206	40	0.13042	0.25	7.3383	2.15	0.40809	2.13	0.99	1.1	4000	1601	2031	158579
n281-25a	weakly zoned, euhedral	2104	3	2115	19	2125	39	0.13046	0.20	7.0245	2.14	0.39051	2.13	1.00		1940	448	906	39170
n281-26a	zoned, euhedral	2108	5	2126	20	2145	40	0.13076	0.27	7.1188	2.20	0.39485	2.19	0.99		306	271	166	55036
N509 Petäjäselkä granodiorite																			
N509-01a	dark zoned rim of rounded zr	2019	153	1767	79	1563	12	0.12428	9.09	4.7012	9.13	0.27435	0.88	0.10		553	145	190	8210
N509-06A	zoned, euhedral	1756	7	1744	12	1734	21	0.10740	0.38	4.5702	1.40	0.30861	1.35	0.96		390	576	186	6200
N509-14A	zoned, euhedral	1798	10	1751	12	1711	20	0.10992	0.58	4.6070	1.45	0.30397	1.32	0.92	-1.8	135	234	67	23491
N509-25A	weakly zoned edge	1786	5	1817	11	1844	21	0.10920	0.27	4.9867	1.34	0.33120	1.32	0.98	0.7	339	116	136	59701
N509-25B	zoned core of euhedral zr	1746	9	1747	12	1748	20	0.10682	0.51	4.5871	1.41	0.31144	1.32	0.93		258	341	117	3705
N509-34A	unzoned, euhedral	1788	9	1805	12	1820	21	0.10930	0.48	4.9150	1.40	0.32614	1.31	0.94		114	111	52	81633

Table 2. cont. Ion microprobe U-Pb data

Sample/ spot	Zircon zoning and morphology*	derived ages $^{207}Pb/^{206}Pb$	±σ	$^{207}Pb/^{235}U$	±σ	$^{206}Pb/^{238}U$	±σ	corrected ratios $^{207}Pb/^{206}Pb$	±σ %	$^{207}Pb/^{235}U$	±σ %	$^{206}Pb/^{238}U$	±σ %	r	Disc.% 2σ lim.	elemental data U ppm	Th ppm	Pb ppm	$^{206}Pb/^{204}Pb$ measured
N509 Petäjäselkä granodiorite																			
N509-38A	zoned, euhedral	1781	13	1777	13	1773	21	0.10890	0.71	4.7545	1.50	0.31665	1.32	0.88		97	92	43	72046
N509-65A	weakly zoned, euhedral	1808	10	1791	12	1776	21	0.11050	0.56	4.8339	1.44	0.31728	1.33	0.92		162	244	81	30855
N509-66a	zoned, euhedral	1782	31	1621	16	1499	11	0.10894	1.73	3.9332	1.92	0.26185	0.84	0.44	-9.6	1046	1707	409	953
N509-66b	zoned, edge	1760	24	1596	13	1475	13	0.10764	1.34	3.8147	1.66	0.25703	0.98	0.59	-11.6	433	683	177	1520
N509-74a	weakly zoned, euhedral	1791	7	1718	9	1659	15	0.10950	0.36	4.4306	1.06	0.29346	0.99	0.94	-5.9	257	498	128	48520
n509-80a	zoned, oval	1754	9	1736	8	1720	13	0.10730	0.52	4.5248	0.99	0.30584	0.84	0.85		111	140	50	36062
N509-84A	weakly zoned, rounded	1729	10	1774	12	1813	21	0.10582	0.55	4.7396	1.43	0.32485	1.32	0.92	1.8	123	169	60	3343
N509-89A	zoned, core	1808	14	1797	13	1788	21	0.11050	0.78	4.8685	1.53	0.31955	1.31	0.86		114	129	53	19908
N509-89B	weakly zoned rim, euhedral	1723	9	1762	12	1795	21	0.10550	0.50	4.6698	1.40	0.32103	1.31	0.93	1.1	171	138	74	65833
N509-94a	zoned, oval	1798	10	1719	9	1654	14	0.10990	0.55	4.4331	1.09	0.29256	0.94	0.86	-5.9	110	122	46	31328
n509-95a	zoned, euhedral	1790	14	1747	10	1711	13	0.10942	0.78	4.5872	1.15	0.30406	0.84	0.73	-1.0	112	132	50	2782
N509-98a	weakly zoned, long prism	1774	9	1710	8	1659	13	0.10847	0.49	4.3899	0.99	0.29353	0.86	0.87	-4.5	140	87	52	8319
n509-100a	weakly zoned, long prism	1809	11	1738	11	1679	18	0.11060	0.62	4.5356	1.34	0.29743	1.18	0.88	-4.6	181	231	80	57703
N509-101a	zoned, long prism	1783	7	1737	8	1699	13	0.10900	0.37	4.5319	0.92	0.30156	0.84	0.91	-3.0	209	72	76	26932
n509-102a	zoned, euhedral	1795	8	1722	8	1662	12	0.10972	0.45	4.4497	0.96	0.29415	0.84	0.88	-5.8	212	207	85	8569
N510 Vääräjärventie granite																			
N510-04a	weakly zoned dark	1774	7	1766	8	1759	13	0.10850	0.40	4.6923	0.94	0.31366	0.85	0.90		95	129	44	73584
N510-04b	weakly zoned, edge	1661	12	1632	9	1610	12	0.10200	0.65	3.9901	1.07	0.28372	0.84	0.79		52	65	21	68399
N510-06a	weakly zoned	1821	7	1767	8	1722	14	0.11130	0.39	4.6976	1.01	0.30611	0.93	0.92	-3.7	198	126	78	97847
N510-08a	unzoned dark	1781	7	1831	8	1875	14	0.10888	0.39	5.0687	0.95	0.33764	0.87	0.91	3.5	166	158	77	25988
N510-09a	zoned	1771	11	1763	10	1757	15	0.10830	0.60	4.6780	1.17	0.31328	1.00	0.86		64	92	30	119346
N510-09b	weakly zoned dark	1567	10	1623	11	1667	18	0.09697	0.56	3.9464	1.33	0.29516	1.21	0.91	3.4	125	64	46	73638
N510-18a	weakly zoned dark	1768	8	1778	9	1788	14	0.10810	0.42	4.7633	1.01	0.31958	0.92	0.91		175	93	70	33568
N510-19a	zoned	1786	9	1740	8	1702	13	0.10920	0.52	4.5484	1.00	0.30209	0.85	0.85	-2.5	97	43	36	39078
N510-20a	weakly zoned	1716	11	1733	9	1747	13	0.10508	0.62	4.5098	1.06	0.31126	0.86	0.81		126	212	63	8439
N510-22a	zoned	1788	12	1775	9	1763	13	0.10930	0.68	4.7411	1.09	0.31460	0.85	0.78		57	72	26	30628
N510-34a	zoned	1783	8	1754	8	1730	13	0.10900	0.44	4.6263	0.95	0.30783	0.84	0.89	-0.7	79	111	37	32415
N510-38a	zoned	1771	8	1758	8	1746	13	0.10830	0.42	4.6465	0.95	0.31117	0.85	0.90		99	240	55	39604

Table 2. cont. Ion microprobe U-Pb data

Sample/	Zircon zoning and	derived ages						corrected ratios							elemental data				
spot	morphology*	$^{207}Pb/^{206}Pb$	±σ	$^{207}Pb/^{235}U$	±σ	$^{206}Pb/^{238}U$	±σ	$^{207}Pb/^{206}Pb$	±σ %	$^{207}Pb/^{235}U$	±σ %	$^{206}Pb/^{238}U$	±σ %	r	Disc.% 2σ lim.	U ppm	Th ppm	Pb ppm	$^{206}Pb/^{204}Pb$ measured
N510 Vääräjärventie granite																			
N510-43a	zoned, edge	1739	14	1788	10	1832	14	0.10640	0.74	4.8204	1.16	0.32859	0.90	0.77	2.1	97	128	47	2899
N510-46a	zoned, euhedral	1811	14	1788	11	1769	16	0.11070	0.75	4.8190	1.29	0.31572	1.04	0.81		48	58	22	13772
N510-48a	zoned, euhedral	1794	14	1778	10	1764	13	0.10970	0.78	4.7612	1.17	0.31478	0.87	0.75		73	110	35	33256
N510-51a	zoned, rounded	1740	27	1647	14	1575	12	0.10649	1.47	4.0640	1.71	0.27678	0.87	0.51	-3.6	60	96	26	3490
N510-54a	zoned, euhedral	1796	14	1846	10	1891	15	0.10980	0.78	5.1613	1.19	0.34092	0.90	0.75	1.9	51	72	26	17428
N510-59a	weakly zoned, euhedral	1778	13	1668	9	1582	12	0.10873	0.74	4.1707	1.12	0.27820	0.84	0.75	-8.7	139	111	52	10718
N510-60a	zoned, euhedral	1759	12	1697	9	1647	13	0.10757	0.65	4.3168	1.09	0.29106	0.87	0.80	-3.7	120	73	45	7047
N511 Petäjäselkä monzogranite																			
N511-02a	zoned, euhedral	1794	36	1496	18	1296	13	0.10966	1.98	3.3655	2.27	0.22259	1.11	0.49	-21.3	178	169	76	60024
N511-02b	weakly zoned edge	1798	33	1656	20	1547	21	0.10994	1.81	4.1099	2.38	0.27113	1.54	0.65	-7.0	346	305	111	249
N511-05a	weakly zoned, euhedral	1788	9	1661	21	1563	34	0.10929	0.50	4.1355	2.52	0.27443	2.47	0.98	-9.3	264	185	106	492
N511-06a	unzoned, long prism	1782	19	1611	12	1483	15	0.10897	1.03	3.8869	1.52	0.25869	1.11	0.73	-13.6	370	304	147	2562
N511-07a	weakly zoned core	1947	9	1781	10	1642	16	0.11938	0.48	4.7751	1.20	0.29011	1.10	0.92	-14.9	578	697	252	4537
N511-08a	weakly zoned, euhedral	1743	37	1522	19	1368	14	0.10663	2.05	3.4751	2.33	0.23637	1.10	0.47	-14.1	1545	443	520	12045
N511-09a	weakly zoned, oval	1874	7	1850	10	1829	17	0.11460	0.38	5.1830	1.15	0.32801	1.09	0.94		124	176	50	1149
N511-09b	weakly zoned edge	1811	5	1773	10	1741	18	0.11071	0.28	4.7321	1.19	0.31001	1.15	0.97	-1.9	136	200	44	293
N511-13a	weakly zoned, oval	1763	16	1727	13	1697	19	0.10785	0.88	4.4778	1.54	0.30111	1.27	0.82		585	157	218	16513
N511-14a	weakly zoned core	1782	46	1485	22	1286	13	0.10898	2.57	3.3168	2.80	0.22073	1.11	0.40	-18.6	2810	3725	1045	128684
N511-15a	weakly zoned core of euhedral zr	1951	11	1809	9	1688	13	0.11965	0.59	4.9387	1.06	0.29935	0.88	0.83	-12.3	109	127	50	123062
N511-15b	weakly zoned dark rim	1781	3	1680	7	1601	12	0.10887	0.16	4.2317	0.86	0.28191	0.84	0.98	-9.7	190	222	85	2675
N511-16a	weakly zoned core of rounded zr	2463	33	2411	22	2350	26	0.16070	1.96	9.7468	2.37	0.43989	1.33	0.56		717	903	299	1139
N511-16b	unzoned rim	1803	5	1694	10	1608	16	0.11019	0.28	4.3049	1.19	0.28335	1.15	0.97	-9.8	655	1221	249	458
N511-17a	weakly zoned, euhedral	1788	10	1766	11	1748	18	0.10932	0.55	4.6940	1.30	0.31141	1.18	0.91		767	186	287	137912
N511-18a	weakly zoned, euhedral	1788	8	1788	10	1787	17	0.10930	0.46	4.8149	1.18	0.31950	1.09	0.92		470	248	161	1450
N511-18b	unzoned dark edge	1798	9	1788	11	1779	19	0.10990	0.49	4.8155	1.29	0.31779	1.20	0.93		904	169	298	9625
N511-26a	weakly zoned, long prism	1792	25	1685	15	1601	16	0.10958	1.39	4.2586	1.78	0.28187	1.12	0.63	-5.3	2236	786	843	22883
N511-28a	weakly zoned dark rim	1842	11	1669	23	1535	37	0.11264	0.59	4.1766	2.80	0.26893	2.73	0.98	-13.5	709	255	225	4564

Table 2. cont. Ion microprobe U-Pb data

Sample/ spot	Zircon zoning and morphology*	derived ages $^{207}Pb/^{206}Pb$	±σ	$^{207}Pb/^{235}U$	±σ	$^{206}Pb/^{238}U$	±σ	corrected ratios $^{207}Pb/^{206}Pb$	±σ %	$^{207}Pb/^{235}U$	±σ %	$^{206}Pb/^{238}U$	±σ %	r	Disc.% 2σ lim.	elemental data U ppm	Th ppm	Pb ppm	$^{206}Pb/^{204}Pb$ measured
N511 Petäjäselkä monzogranite																			
N511-28b	weakly zoned core of euhedral zr	1733	7	1738	10	1742	17	0.10610	0.36	4.5378	1.15	0.31019	1.09	0.95		338	200	142	76864
N511-32a	weakly zoned, euhedral	1776	5	1734	11	1700	19	0.10860	0.27	4.5190	1.31	0.30179	1.28	0.98	-2.1	100	83	38	4032
N511-33a	zoned, euhedral	1774	10	1718	10	1672	16	0.10849	0.57	4.4306	1.23	0.29619	1.09	0.89	-3.2	190	159	74	730
N511-38a	unzoned dark rim, euhedral	1784	4	1773	10	1764	17	0.10908	0.24	4.7321	1.13	0.31464	1.11	0.98		523	8	268	349040
N512 Tohmo monzogranite																			
N512-01a	zoned, euhedral, edge	1760	7	1905	13	2042	26	0.10764	0.37	5.5313	1.53	0.37269	1.49	0.97	14.8	360	283	173	2494
N512-08a	zoned, euhedral	1654	7	1411	9	1255	13	0.10165	0.39	3.0124	1.18	0.21493	1.12	0.94	-24.0	274	400	91	13098
N512-14a	weakly zoned, euhedral	1824	66	1534	33	1332	20	0.11152	3.71	3.5282	4.07	0.22947	1.68	0.41	-12.7	222	303	73	154
N512-17a	weakly zoned dark, euhedral	1792	3	1853	8	1908	14	0.10958	0.18	5.2046	0.89	0.34448	0.87	0.98	5.4	2864	101	1106	42212
N512-19a	zoned, euhedral	1825	10	1772	10	1727	17	0.11157	0.53	4.7268	1.21	0.30727	1.09	0.90	-2.9	183	236	80	2210
N512-21a	zoned, euhedral	1776	8	1752	8	1732	13	0.10863	0.45	4.6159	0.99	0.30819	0.89	0.89	-0.1	385	207	147	5727
N512-25a	zoned, euhedral, edge	1780	8	1260	7	978	8	0.10881	0.43	2.4581	0.97	0.16384	0.87	0.90	-46.2	238	286	60	17153
N512-36a	zoned, euhedral, edge	1803	6	1726	9	1663	16	0.11022	0.34	4.4720	1.14	0.29427	1.09	0.95	-6.3	243	279	101	6845
N512-38a	zoned, euhedral	1775	11	1826	9	1872	14	0.10852	0.59	5.0419	1.06	0.33696	0.88	0.83	2.9	215	314	110	1894
N512-39a	weakly zoned, oval, edge	1732	29	1743	15	1753	14	0.10599	1.61	4.5676	1.83	0.31254	0.88	0.48		164	117	65	981
N512-42a	zoned, euhedral, edge	1795	9	1806	9	1815	14	0.10973	0.49	4.9213	1.03	0.32528	0.91	0.88		147	137	65	20292
N512-45a	weakly zoned, euhedral, edge	1779	7	1889	13	1991	26	0.10879	0.38	5.4265	1.56	0.36178	1.51	0.97	9.9	3781	164	1532	3226
N512-46a	weakly zoned, euhedral	1716	9	1632	14	1567	23	0.10507	0.51	3.9871	1.72	0.27521	1.64	0.96	-5.9	257	284	101	7474
N512-51a	zoned, oval, edge	1790	8	1905	13	2012	26	0.10942	0.42	5.5274	1.55	0.36639	1.49	0.96	10.5	232	276	119	23261
N512-61a	zoned, oval, edge	1803	9	1895	13	1980	25	0.11024	0.47	5.4647	1.56	0.35954	1.49	0.95	7.4	137	225	75	20433
N512-64a	zoned, long prism	1772	12	1805	14	1833	24	0.10837	0.65	4.9137	1.62	0.32885	1.49	0.92		252	363	124	5596

All errors are at 1 sigma level. Degree of discordance is calculated at the closest 2 sigma limit.

*) Analysed zircon domain: zoned = zoning in BSE and CL images; the terms core and rim are for separate cores and overgrowth rims if they can clearly be observed from BSE images.

If not specially mentioned the analysed spot is from the interior of the zircon grain.

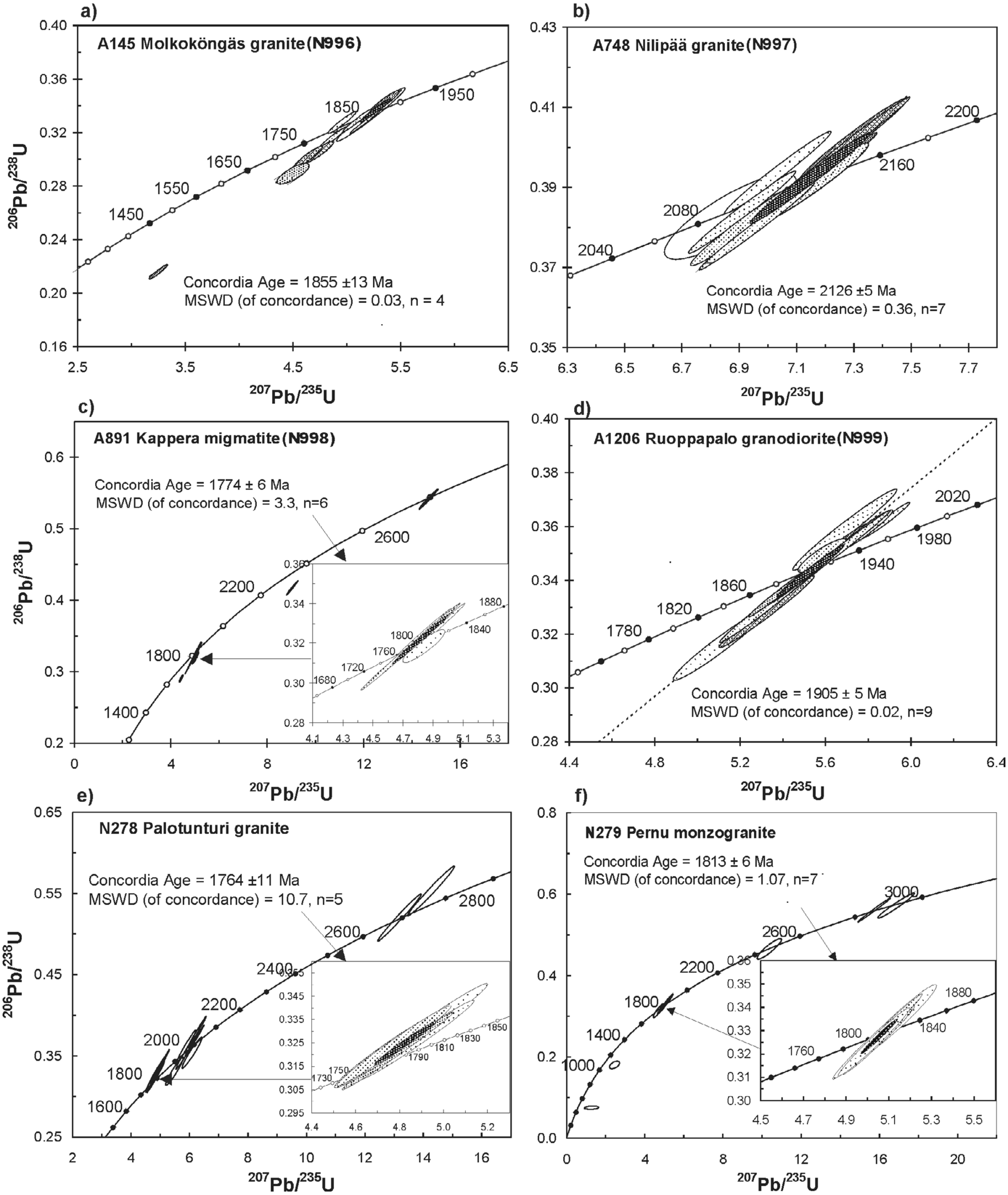

Fig. 4. Concordia plots of zircons analysed using the ion microprobe. Data point error ellipses are 2σ.

Table 3. U-Pb data on zircons from the Jääskö monzonite and the Nilipää granite

Sample information	Sample	U	Pb	$^{206}Pb/^{204}Pb$	$^{208}Pb/^{206}Pb$	ISOTOPIC RATIOS*						r**	APPARENT AGES / Ma		
density, size (mesh), a16h (abraded 16h)	weight / mg	ppm	ppm	measured	radiogenic	$^{206}Pb/^{238}U$	$2\sigma_m$%	$^{207}Pb/^{235}U$	$2\sigma_m$%	$^{207}Pb/^{206}Pb$	$2\sigma_m$%		$^{206}Pb/^{238}U$	$^{207}Pb/^{235}U$	$^{207}Pb/^{206}Pb$
A1714 Jääskö monzonite															
A1714D +4.3 +200 a16h	0.44	83.2	33.6	12233	0.35	0.31919	0.5	4.833	0.5	0.10981	0.1	0.98	1786	1791	1796
A1714E +4.3 +200	0.48	104	41.1	5838	0.33	0.31626	0.5	4.781	0.5	0.10964	0.1	0.98	1771	1782	1793
A1714F +4.3 +200 a16h	0.51	102	40.9	3543	0.35	0.31914	0.5	4.833	0.55	0.10984	0.2	0.93	1786	1791	1797
A1714G +4.3 +100 a15h	0.49	92	37.5	2437	0.36	0.31843	0.5	4.815	0.55	0.10967	0.2	0.93	1782	1788	1794
A1708 Iso Nilipää granite															
A1708A +4.2	0.44	663	273	1943	0.17	0.35698	0.5	6.463	0.5	0.13130	0.1	0.97	1968	2041	2115

*) Isotopic ratios corrected for fractionation, blank (Pb 50 pg) and age related common lead (Stacey & Kramers 1975).

**) Error correlation for 207Pb/235U vs. 206Pb/238U ratios.

A748 Nilipää granite (N997)

In the +4.6 gcm^{-3} density fraction most of the zircons of the Nilipää sample are transparent, long prismatic (Fig. 4) and quite fine-grained. Zircons in other fractions, 4.6 – 4.2 gcm^{-3} / +100 mesh and 4.2 – 4.0 gcm^{-3} were similar to those in the heaviest fraction. Zircons are mostly zoned and contain abundant inclusions. A few small, altered or recrystallised core domains have been detected (Fig. 3c). The uranium concentration varies between 1398 and 34 ppm. The lowest, exceptional value of 34 ppm was measured from a possible metamorphic zircon type (09a, Table 2).

The obtained age data are concordant (Table 2). When excluding the anomalous analysis 09a, the data give a concordia age of 2126 ± 5 Ma (Fig. 4b). The difference between the oldest and the two youngest ages is insignificant. The ion microprobe age is, within the error limits, the same as the conventional TIMS age of 2136 ± 5Ma (Huhma, 1986; Rastas et al., 2001).

One TIMS U-Pb analysis made on long euhedral zircons from sample A1708 plots exactly on the chord defined by the three analyses from the original sample A748 (Table 3). The four analyses from these two samples define a line, which intercepts the concordia curve at 2134 ± 4 Ma and 357 ± 33 Ma (MSWD=0.6).

A891 Kappera migmatite (N998)

In the 4.2 – 4.0 gcm^{-3} fraction, the rather fine-grained zircon grains (-100mesh) mostly form very bright and transparent, thin, long needles, apart from a few brown, shorter and thicker prismatic grains. In the grain-size fraction +100 mesh (> 160 µm), the zircons are more heterogeneous. The BSE images from the Kappera zircons commonly exhibit slight to heavy alteration with thin fractured rim around the crystals, older altered and recrystallised cores, thin zoning or unzoned large domains. Only a few non-altered crystals with narrow oscillatory zoning have been detected.

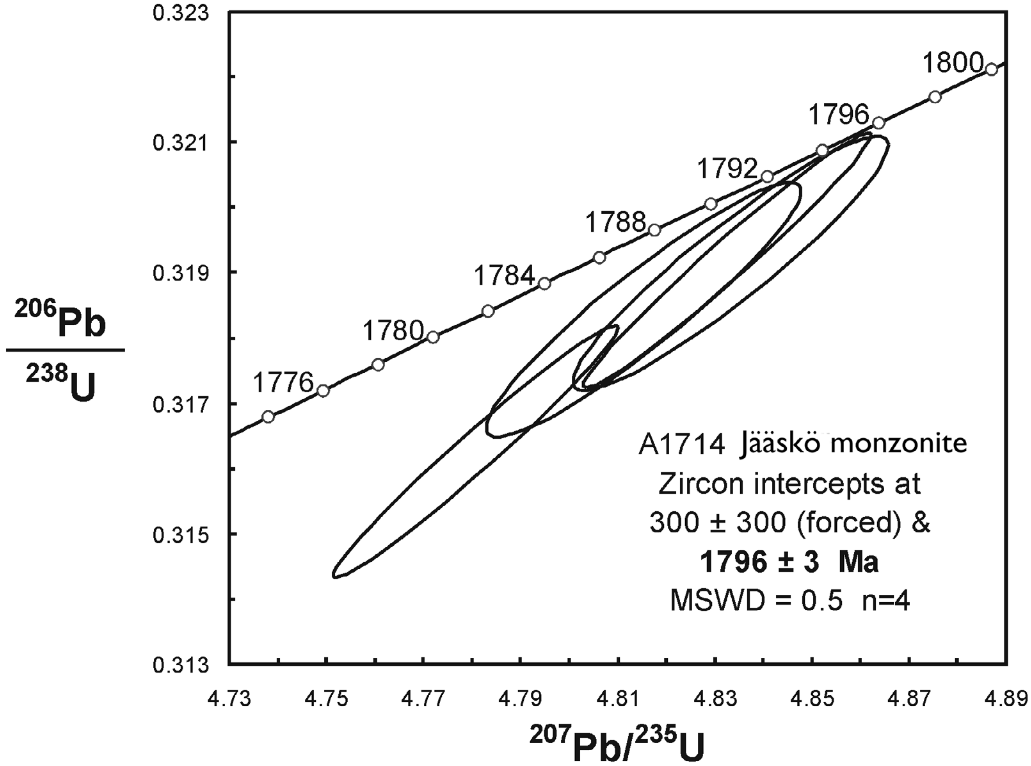

Fig. 5. Concordia plot of zircons from the Jääskö monzonite analysed using TIMS.

Most zircons give an age of ca. 1.8 Ga, one analysis being discordant. The six concordant analyses give a concordia age of 1774 ± 6 Ma (Fig. 4c), which is considered as a good approximation for the age of the melting event that produced the leucosome. This age is exactly the same as the U-Pb age on titanite from the same sample (Mänttäri, 1995). Both the long needle-like and shorter grains (Fig. 3e) give the same age. One Archaean grain with an age of 2.78 Ga was found (Fig. 3d, n998-02a) and one slightly discordant grain yielded a $^{207}Pb/^{206}Pb$ age of 2.39 Ga (Table 2 and Fig. 4c). This grain is morphologically and internally quite similar to two other grains (03a and 04a), which yielded ages of ca. 1.8 Ga. A plausible interpretation is that these unzoned domains represent metamictic and recrystallised older grains, in which case many zircons in the leucosome would be inherited, except for the long oscillatory-zoned zircons, which would represent crystallisation from melt. One zircon gives a concordant age of 1.07 Ga (07a in Table 2), which probably represents accidental modern contamination. The Sm-Nd analysis provides an initial ε_{Nd}-value of -8.5, which is consistent with the presence of Archaean material in the protolith (Table 4).

A1206 Ruoppapalo granodiorite (N999)

In the Ruoppapalo sample zircon grains are elongate, brown, euhedral and prismatic, with a rather uniform grain-size distribution. In BSE images os-

Table 4. Sm-Nd isotopic data.

Sample	Location	Map coordinates northing	Map coordinates easting	Rock type	Sm (ppm)	Nd (ppm)	$^{147}Sm/^{144}Nd$ (±0.4%)	$^{143}Nd/^{144}Nd$	$2\sigma_m$	T (Ma)	eps(T)	T_{DM}(Ma)
PSH-01-37	Molkokönġäs	7441745	2547221	granite	3.91	31.45	0.0751	0.510816	0.000010	1800	-7.6	2445
PSH-01-40	Lehmikari	7448521	2546043	syenodiorite	19.61	118.80	0.0998	0.511184	0.000010	1800	-6.1	2485
PSH-01-42.1	Molkokönġäs	7442086	2546811	quartz monzonite	8.77	59.39	0.0893	0.511097	0.000010	1800	-5.4	2379
PSH-01-45.4	Jääskö	7438834	2547969	quartz monzonite dyke	3.65	29.74	0.0742	0.510931	0.000010	1800	-5.1	2302
PSH-01-47.1	Taljasuvanto	7436863	2549223	granodiorite gneiss	6.30	36.59	0.1041	0.511159	0.000010	1800	-7.6	2621
PSH-01-49.1	Ranta-Äijövaara	7435108	2551673	granite, leucosome	3.54	26.82	0.0798	0.510829	0.000010	1800	-8.4	2516
PSH-01-49.2	Ranta-Äijövaara	7435108	2551673	mica gneiss	6.72	48.72	0.0834	0.510730	0.000020	1800	-11.2	2700
PSH-01-51	Maununmatti	7388090	3448657	granite	9.27	58.03	0.0966	0.511135	0.000010	1800	-6.3	2481
PSH-01-56.1	Palo	7410370	2564441	granite	6.16	56.55	0.0658	0.510715	0.000010	1800	-7.4	2394
PSH-01-56.2	Palo	7410370	2564441	quartz monzonite	3.64	29.61	0.0743	0.510780	0.000020	1800	-8.1	2470
PSH-01-61.1	Marraskoski	7411875	2562522	granite	2.12	19.50	0.0658	0.510713	0.000010	1800	-7.5	2395
A1206 (2)	Ruoppapalo	7550950	3444100	granodiorite	1.29	7.11	0.1097	0.511468	0.000014	1905	-1.7	2309
A145 (1)	Molkokönġäs	7440549	2547349	granite	3.25	29.61	0.0664	0.510710	0.000031	1843	-6.9	2412
A1665	Tainio	7451621	2538883	gabbro	3.11	17.17	0.1094	0.511353	0.000011	1796	-5.1	2467
A1714	Jääskö	7438834	2547969	monzonite	12.88	87.95	0.0885	0.511120	0.000010	1796	-4.8	2336
A355	Käkkälöjoki	7591450	2505599	granite	3.71	30.03	0.0747	0.510845	0.000010	1800	-6.9	2406
A748 (1)	Iso Nilipää	7493749	2555019	granite	3.96	26.40	0.0908	0.511021	0.000020	2136	-2.6	2509
A891	Kappera	7585499	2526799	granite	7.23	54.85	0.0797	0.510843	0.000010	1780	-8.4	2498
N278	Palotunturi	7387849	4451799	granite	2.45	19.39	0.0769	0.510852	0.000011	1764	-7.9	2430
N279	Pernu	7350750	3522500	monzogranite	1.26	11.32	0.0677	0.510850	0.000008	1813	-4.9	2280
N280	Jumisko	7362760	3549170	monzogranite	1.82	16.43	0.0674	0.510814	0.000015	1761	-6.5	2310
N281	Tohmo	7409620	3515640	granodiorite	2.36	17.27	0.0834	0.511000	0.000032	2105	-1.4	2380
N509	Petäjäselkä	7379830	3534650	granodiorite	12.27	71.00	0.1052	0.511158	0.000010	1790	-8.0	2640
N510	Vääräjärventie	7368252	3564102	granite	10.72	74.32	0.0878	0.510949	0.000013	1771	-8.4	2530
N511	Petäjäselkä	7379830	3534650	monzogranite	1.89	19.55	0.0590	0.510704	0.000008	1790	-6.2	2290
N512	Tohmo	7409620	3515640	monzogranite dyke	2.80	16.67	0.1021	0.511124	0.000009	1789	-7.9	2620

(1): Huhma, 1986; (2): Hanski & Huhma, 2005.

For samples with unknown age the epsilon has been calculated using an age of 1800 Ma cillatory zoning attributed to magmatic crystallisation is visible in most grains though in some zircons this is not so obvious (Figs 3f-h). The twelve analyses (Table 2) yield an upper intercept age of 1905 ± 7 Ma (MSWD=2.5, n=12), and nine concordant analyses give a concordia age of 1905 ± 5 Ma (Fig. 4d). The unzoned rim of zircon n999-02 may represent a metamorphic overgrowth, but the age of 1894 ± 24 Ma is statistically indistinguishable from the magmatic age of 1905 ± 5 Ma. A distinctive feature of all zircons from the Ruoppapalo granodiorite is the low Th/U-ratio of ca. 0.2.

Palotunturi granite (N278)

The Palotunturi sample was taken from a grey, medium grained deformed granite. The sample provided only a few zircons andthey were classified into three types based on their morphology. The first type consists of euhedral, long, transparent and weakly zoned, 140 – 250 µm grains which are brownish to colourless, and have a length/width ratio of 2.5 – 3.5:1. The zircons of the second type are 140 – 180 µm in size, subhedral, oval, mostly transparent, light brown to bright and colourless. The length/width ratio is around 2:1. These zircons have weakly zoned interiors with generally thin, < 30 µm overgrowth rims. The third type of zircons are small, < 150 µm in size, oval, light brown and transparent. Some of them have a weakly zoned core and an unzoned rim.

The zircons from the Palotunturi granite show three age groups that correspond well to the morphological types. Two of the analysed 14 spots have Archaean ages of 2.7 Ga. These represent the small (< 150 µm) and oval zircons (type III) and both of them have younger rims (Fig. 6), one of which has a $^{207}Pb/^{206}Pb$ age of 1761 ± 6 Ma (n278-20b, Fig. 6a) and another 2025 ± 22 Ma (n278-24b, Table 2). The 2.03 Ga age result of the zircon rim 24b may represent a mixture of the Archaean core and 1.75 – 1.77 Ga rim. Four grains have $^{207}Pb/^{206}Pb$ ages from 1928 ± 16 Ma to 1977 ± 6 Ma. These grains are oval and they have narrow outer rims, which may represent metamorphic overgrowths (type II, Fig. 6b). From one zircon the overgrowth gives approximately the same age as the interior (n278-04a and n278-04b in Table 2). The remaining five analyses are from interiors of idiomorphic, oscillatory zoned zircons (type I) that give a concordia age of 1764 ± 11 Ma (Fig. 4e), which, on the basis of the morphology represents the age of the magmatic crystallisation of the intrusion, the older zircons being inherited. The ε_{Nd}(1.76 Ga) of the Palotunturi granite is -7.9 ± 0.3 (Table 4, Fig. 7).

Pernu monzogranite (N279)

The Pernu sample contained relatively few zircons, which were divided into three types on the basis of their morphology and colour. Zircons of the first type are often euhedral, elongated and zoned, partly transparent and light brown to colourless. Their size varies between 170 – 400 µm and the length/width ratio is 3:1. The second type of zircon is characterised by roundish, light brown to colourless, mainly subhedral and anhedral grains, varying in size from 140 – 350 µm, and commonly having thin overgrowth rims. Zircons of the third type tend to be elongated, brown, partly transparent, mainly subhedral and euhedral. The grains range from 160 – 490 µm in size and their length/width ratio from 2-3.5:1.

Two of the twelve ion-probe analyses from the Pernu sample yielded very low $^{206}Pb/^{204}Pb$ ratios and therefore could not be used for dating. The other data are concordant. The Pernu monzogranite has two zircons with an age of ca. 2.9 Ga (08a and 48a, Table 2 and Fig. 6d) and one zircon dated at 2.5 Ga (30a, Table 2). Morphologies do notdirectly correlate with the ages. One of these older ages is from the interior of an elongated, type III zircon grain and two from the interiors of oval shaped type II grains. These oldest zircons have a weakly zoned core and a metamict overgrowth rim. Neglecting the discordant analyses with high errors, all other zircons have $^{207}Pb/^{206}Pb$ ages of 1809 – 1819 Ma. They are mostly roundish, type II zircons but one type I elongated zircon was also in this age group. The concordia age for seven concordant analyses is 1813 ± 6 Ma (Fig. 4f). This age represents the emplacement and crystallisation of the in-

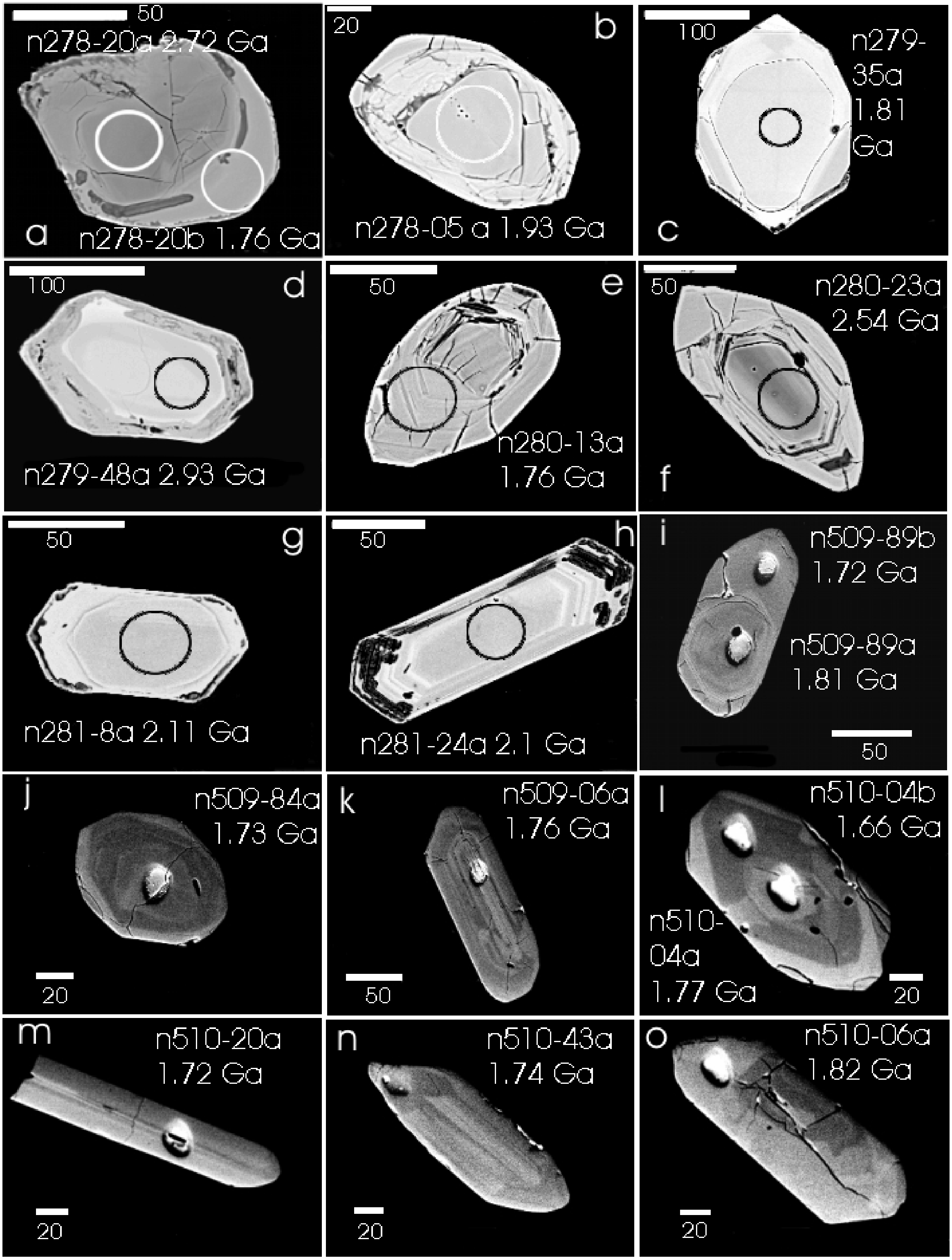

Fig. 6. BSE images of zircons. The number at the scale bar refers to microns.

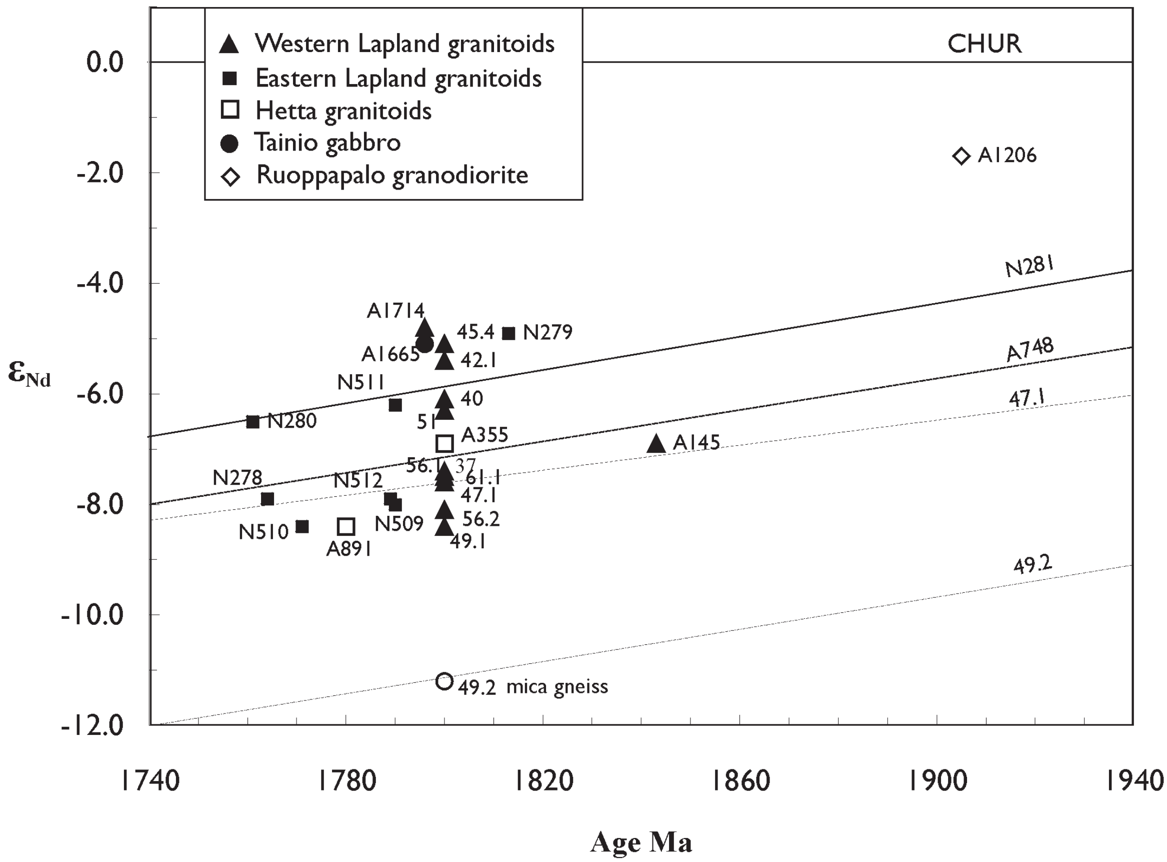

Fig 7. ε_{Nd} vs. age diagram showing initial ε-values for Proterozoic granitoids in Finnish Lapland (Table 2). For samples with unknown age the epsilon has been calculated using an age of 1800 Ma. Evolution lines are shown for the two ca. 2.1 Ga granitoids (A748, N281), and the gneisses related to the W-Lapland granitoids (47.1, 49.2). For the W-Lapland granitoids the prefix "PSH-01-" is not shown. CHUR= Bulk Earth (ε=0 by definition).

trusion. The Sm-Nd analysis on a whole rock sample gives an initial ε_{Nd} value of -4.9 at 1.81 Ga (Table 4).

Jumisko monzogranite (N280)

The sample contained abundant zircon grains, which were classified into three types on the basis of morphology and colour. In the first group, zircons are short, subhedral, strongly zoned, brownish and transparent. Their size is 110 – 140 µm and the length/width ratio is 1.5 – 2:1. Zircons of the second type are long, subhedral and anhedral, transparent, light brown and optically zoned, ranging in size from 120 – 170 µm and with length/width ratios of 2.5 : 1. Some zircons have weakly zoned cores surrounded by zoned edges. The third type of zircons is euhedral, long, strongly zoned, brown and transparent; grain size varies from 160-200 µm and length/width ratio is 3.5 : 1.

One slightly discordant analysis (23a) from the Jumisko monzogranite gives a $^{207}Pb/^{206}Pb$ age of 2.5 Ga (Table 2 and Fig. 6f). Thisanalysis is from a weakly zoned interior of a type II zircon whose margin is optically strongly zoned. Seven of the other eight analyses are concordant or nearly concordant at ca. 1.76 Ga, and if all eight are regressed together they provide concordia intercepts at 1756 ± 5 Ma and 184 ± 150 Ma (MSWD=1). For the five concordant analyses the

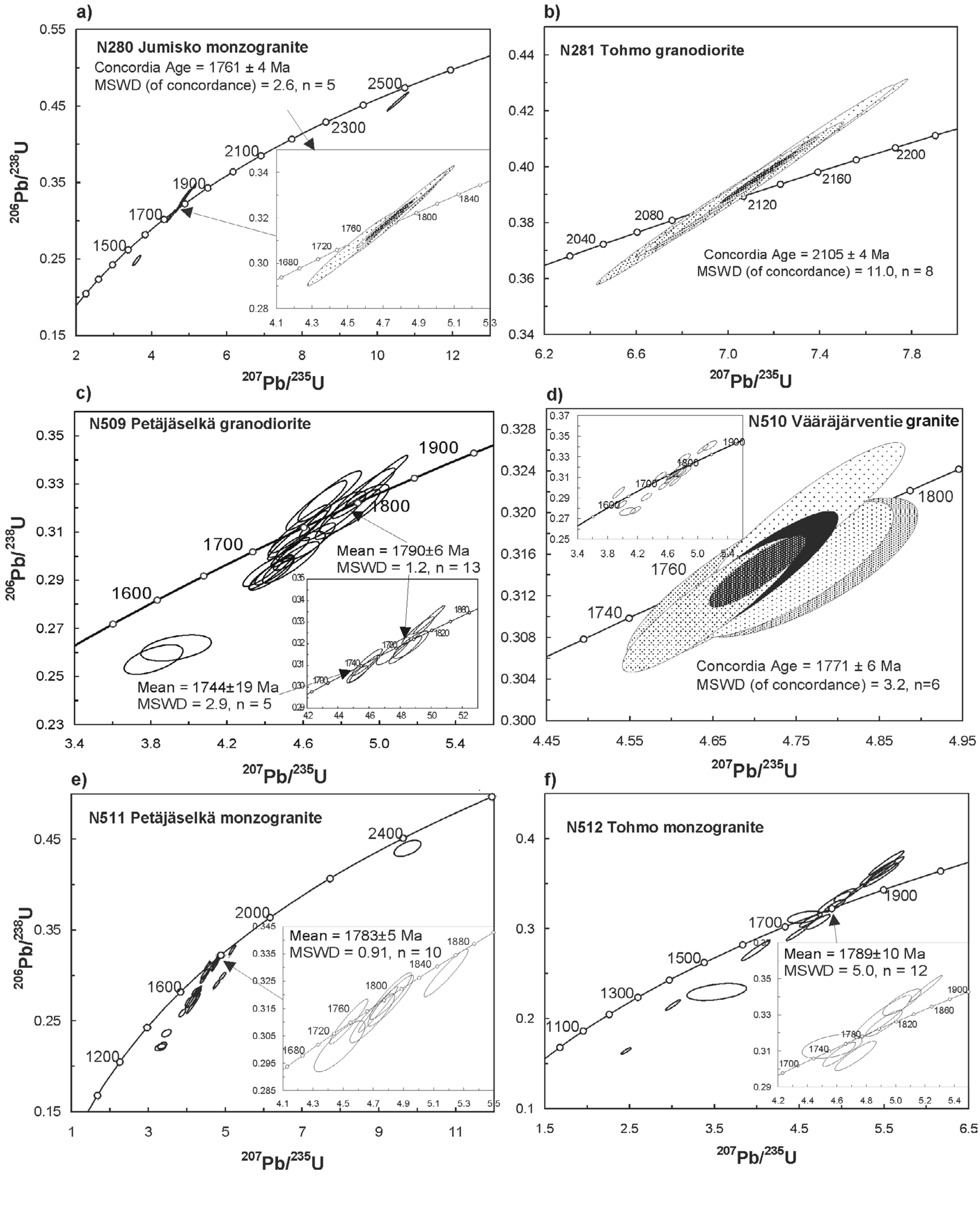

Fig. 8. Concordia plots of zircons analysed using the ion microprobe. Data point error ellipses are 2σ.

concordia age is within error limits the same, 1761 ± 4 Ma (Fig. 8a). Magmatic oscillatory zoning is typical for almost all zircons in this rock (Figs. 6e-f), and the 1760 Ma age can therefore be regarded as the magmatic age of the Jumisko monzogranite. The initial ε_{Nd}(1.76 Ga) for this rock is -6.5 (Table 4).

Tohmo granodiorite (N281)

The Tohmo sample was zircon-poor and the zircon is partly metamictic. Zircon crystals were grouped into three morphologies. Zircons belonging to the first type are transparent, elongated (150 – 200 µm) and in some cases euhedral and zoned (Fig. 6g-h). Some zircon grains in this group also have narrow overgrowth rims. The second group of zircons are brown, elongated (180 – 200 µm) and sometimes zoned. The third type of zircon is roundish and brownish, 100 – 150 µm in size. Most grains in this group are zoned and partly euhedral. Some grains have metamictic margins (Fig. 6h).

All zircons from the Tohmo granodiorite provide concordant analyses at 2.1 Ga regardless of their morphology. The eight analyses give a concordia age of 2105 ± 4 Ma (Fig. 8b), whichis evidently the magmatic age of the intrusion. The initial $\varepsilon_{Nd}$is -1.4 ± 0.6 and the corresponding model age (T_{DM}) 2.38 Ga (Table 4).

Tohmo monzogranite (N512)

The sample N512 from the Tohmo monzogranite was zircon-poor. Zircon crystals can be divided into three main morphological groups. Zircons of the first group are small (< 150 µm), roundish and light in colour; some grains are euhedral and zoned. The second group zircons are larger (ca. 150 – 250 µm) and darker, oval, partly euhedral and zoned. Zircons of the third group are darker than the others and grains are anhedral and generally not zoned, although some crystals have a distinct core.

Due to a low $^{206}Pb/^{204}Pb$ ratio and large error, one of the sixteen ion probe analyses made on the Tohmo monzogranite was rejected (n512-14a, Table 2). Two analyses are highly discordant and some are reversely discordant. Regression of all data yields intercept ages of 126 ± 140 Ma and 1780 ± 22 Ma, and the MSWD of 26 suggests some scatter in excess of analytical error.

Excluding the three most discordant analyses an average $^{207}Pb/^{206}Pb$ age of 1789 ± 10 Ma can be calculated (Fig. 8f). This age is considered as the best estimate for the crystallisation of the Tohmo monzogranite dykes, as most zircon grains have clear magmatic zoning. The reason for the slight heterogeneity is not obvious from the morphology of zircon. The Nd analysis on whole rock sample yields an initial ε_{Nd}(1.79 Ga) value of -7.9.

Petäjäselkä granodiorite (N509)

The sample contained abundant zircon grains, which were divided into four types on the basis of morphology and colour. The first type of zircon is elongated and light brown to brown in colour. Grains are euhedral, zoned and range in size from 150 – 250 µm. The second type of zircon is brown, roundish, partly zoned and 100 – 150 µm in size. The third type is light brown, transparent, roundish, partly zoned and 100 – 150 µm in size. The fourth type of zircon is elongated, 200 – 300 µm in size, generally euhedral, often zoned and transparent to light brown in colour.

After rejecting three analyses, which are discordant or have high errors, the remaining 18 data points are mostly concordant or slightly discordant (Table 2, Fig. 8c). They show a scatter of $^{207}Pb/^{206}Pb$ ages from 1723 ± 18 Ma to 1809 ± 22 Ma and provide an average $^{207}Pb/^{206}Pb$ age of 1778 ± 12 Ma. The MSWD of 7.7 suggests some scatter in excess of analytical error. However, ages do not show any obvious correlation with morphology. The two youngest, 1.72 – 1.73 Ga ages are from the rim (89B) of a euhedral grain that has an older core (89A), and another from the center of a roundish, weakly zoned grain (84A, Figs 6i-j). Rejecting five analyses, which have $^{207}Pb/^{206}Pb$ ages younger than 1.76 Ga, the remaining 13 (less than 5 % discordant) analyses give an average $^{207}Pb/^{206}Pb$ age of 1790 ± 6 Ma, which is interpreted as the crystallisation age of the pluton. The five youngest analyses give an average $^{207}Pb/^{206}Pb$ age of 1744 ± 19 Ma (Fig. 8c). The Sm-Nd analysis on whole rock reveals a relatively high level of REE. The initial ε_{Nd}(1.79 Ga) is -8.0, and clearly shows that the bulk of the REE were derived from much older crustal sources.

Petäjäselkä monzogranite (N511)

The sample contained a lot of zircons, which were divided into three types. The first type consists of euhedral, elongated and narrow grains with sharp edges. They are mainly brown, rarely colourless, and some of them are zoned. The length of the zircons is 160 – 300 µm and the length/width ratio is 4 – 6:1. The second type of zircons are brown to light brown and zoned; they vary in size from 120 – 190 µm, with a length/width ratio around 2:1 and have darker rims overgrowing the inner cores. The third type consists of elongated zircons that are larger than the first and second type zircons, their size being 180 – 300 µm. They are yellowish brown to colourless and partly zoned.

In spite of slight discordance, the bulk of the twenty-three zircon analyses made on the Petäjäselkä monzogranite suggest ages close to 1.79 Ga (Table 2). However, four analyses are significantly older. These includeone zircon core with a $^{207}Pb/^{206}Pb$ age of 2463 Ma (n511-16a, Fig. 8). The rim of this grain gives a slightly discordant analysis with $^{207}Pb/^{206}Pb$ age of 1803 ± 10 Ma (16b). One concordant analysis (n511-09a) gives an age of 1874 ± 14 Ma, whereas the analysis on the outer domain of this grain gives a $^{207}Pb/^{206}Pb$ age of 1811 ± 10 Ma (Fig. 9a). The youngest concordant age of 1733 ± 14 Ma (n511-28B) is from the core of a zircon that has older rim (28A, Table 2). If not meaningless, this spot may represent metamorphic recrystallisation of a previously metamict grain domain, illustrating the inherent difficulties involved in dating such grains. The other analyses with a discordance less than 5 % yield an average $^{207}Pb/^{206}Pb$ age of 1783 ± 5 Ma (Fig. 8e). The heterogeneity of the ages in this rock represents melting of the sedimentary source, which already had a heterogeneous zircon population. Melting and crystallisation took place at around 1.79 Ga. The Sm-Nd analysis on whole rock yields an initial ε_{Nd}(1.79 Ga) is -6.2.

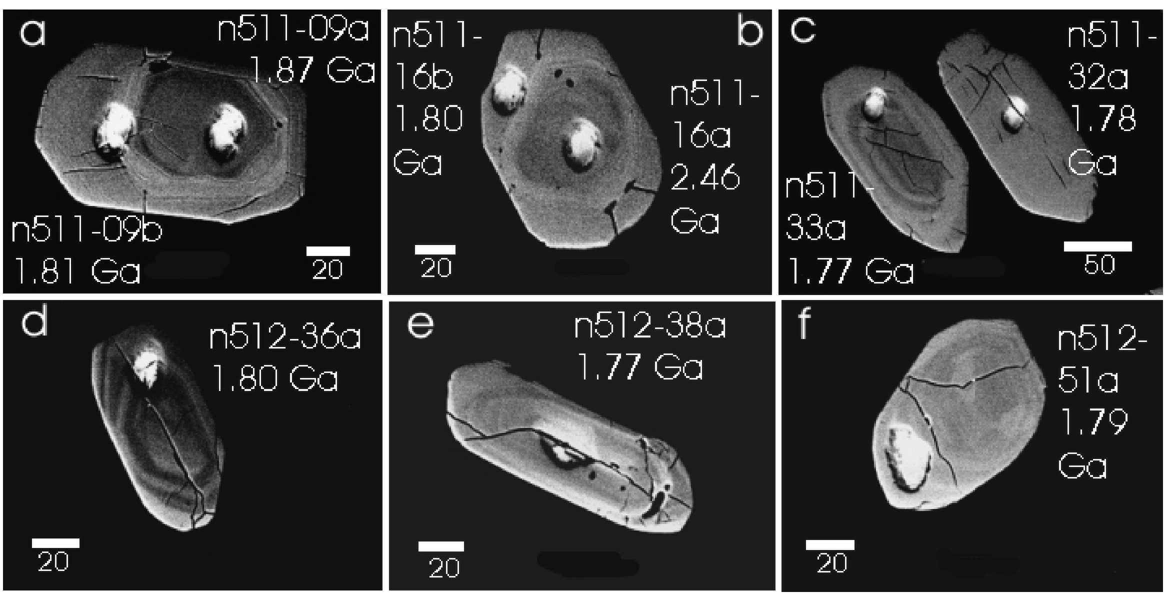

Fig. 9. BSE images of zircons. The number at the scale bar refers to microns.

Vääräjärventie granite (N510)

The Vääräjärventie specimen has abundant zircon. Most zircons are very elongated and transparent, and were divided into three morphological and colour types. The first type of zircons are long (> 200 μm), narrow, oscillatory zoned and some of them have sharp edges. The second type zircons are shorter (< 150 μm), zoned and mainly euhedral. The length/width ratio is smaller than in the first group. Zircons of the third type are darker, larger and not as euhedral as zircons in the first and second group, and they also have inclusions.

All nineteen analyses from zircons in the Vääräjärventie granite are technically good, and mostly provide concordant or nearly concordant results. However, surprisingly young ages were obtained from two zircon rims, which give $^{207}Pb/^{206}Pb$ ages of 1567 Ma (n510-09b) and 1661 Ma (n510-04b, Fig. 6l). These are not very discordant and may indicate late open system behaviour of the U-Pb system. Two zircons that belong morphologically to the type II have $^{207}Pb/^{206}Pb$ ages of 1811 ± 28 Ma and 1821 ± 14 Ma (46a and 06a, Fig. 6o). One interior of the type I zircon gives a $^{207}Pb/^{206}Pb$ age of 1716 ± 22 Ma (20a, Fig. 6m) and two zircon rims 1739 ± 28 and 1740 ± 52 Ma (43a and 51a); each of these grains have typical magmatic zoning (Fig. 6n). All other zircons have $^{207}Pb/^{206}Pb$ ages of 1759 – 1796 Ma regardless of morphology, and these yield an average $^{207}Pb/^{206}Pb$ age of 1781 ± 10 Ma (n=16). Six concordant analyses give a concordia age, which is within error limits the same, 1771 ± 6 Ma (Fig. 7d). Most zircons have a magmatic-type zoning and this age could be considered as the magmatic crystallisation age, although the younger zircons also have magmatic structures, which could indicate an even younger emplacement age, at around 1.72 – 1.74 Ga. This granite has relatively high concentration of REE, the initial ε_{Nd}(1.77 Ga) being -8.3, which together imply derivation from old crustal sources.

6. Discussion

The Sm-Nd data reveal that all 1.84 – 1.77 Ga granitoids in the Central Lapland Granitoid Complex and the Hetta granites (Fig. 1) have strongly negative ε_{Nd}(1.8 Ga), ranging from -8 to -5 (Fig. 3). The corresponding model ages, T_{DM} range from 2.3 to 2.6 Ga (according to the model by DePaolo, 1981). The REE trend estimated from the Sm/Nd ratio is typically steeper than in many estimates of post-Archaean average crustal composition (PAAS; Taylor & McClennan, 1985). Consequently, the Sm-Nd model ages do not represent the average age of the protoliths, but tend to give ages that are too young. Nevertheless, it is evident that these rocks have a major Archaean component in their source,which is also confirmed by the presence of Archaean zircons in some of our samples. This supports the idea of the intracratonic Proterozoic history of the Central Lapland area where most Proterozoic formations are obviously underlain by the Archaean bedrock (Hanski, 2001). Apart from the Ruoppapalo granodiorite, all rocks analysed in this study follow roughly the same Nd evolutionary trend (Fig. 7) which, together with the wide scatter of the granitoid ages, indicates repeated reworking of the crust in intracratonic environment with very little juvenile magmatic input since 2.1 Ga. Even the appinitic lithologies are characterised by low initial ε_{Nd} values (Table 4, Fig. 7), suggesting major interaction of mantle-derived magma with crustal material.

The Ruoppapalo granodiorite is more juvenile having a younger model age than the 1.84 – 1.77 Ga granites, but it is located inside the Kittilä allochthon and may therefore have originated in a different tectonic setting, juxtaposed later with the other formations. The Ruoppapalo granodiorite is located ca. 50 km from the SW contact of the Lapland Granulite Complex. This area south and southwest of the Lapland Granulite Complex has structural trends similar to those in the granulites (Krill, 1985; Tuisku & Huhma, 1998; Nironen & Mänttäri, 2003; Hölttä et al., 2007), an hence they could have been deformed simultaneously with the granulites in the Lapland-

Kola collision at 1.9 Ga. As with the Nilipää granite, the Ruoppapalo pluton is only weakly deformed, implying either that the effect of the Lapland-Kola orogen did not extend to the Ruoppapalo area, or that the emplacement of the Kittilä allochthon took place later than the Lapland-Kola orogen. Alternatively, the weak deformation may also indicate deformation partitioning around the rigid granite, or cessation of compressional tectonics in this area by ca. 1905 Ma.

The Nilipää and Tohmo intrusions represent the oldest dated Palaeoproterozoic granitoids in the Central Lapland Granitoid Complex. Because of the weak deformation of the Nilipää granite, the 2.13 Ga ion probe age was not expected, since the rock cannot be distinguished from the 1.82 – 1.77 Ga granitoids on the basis of structural relationships. During later deformation the Nilipää intrusion has evidently behaved as a rigid body and deformation has partitioned into its country rock. Several mafic intrusions of ca. 2.15 – 2.11 Ga age are present in Central Lapland (Hanski et al., 2001a; Räsänen & Huhma, 2001; Manninen et al., 2001) which may suggest simultaneous underplating of mafic magmas and subsequent melting of the Archaean lower crust, producing the granites, as indicated by the negative ε_{Nd} value of the Nilipää and Tohmo intrusions. The 2.15 – 2.11 Ga magmatism is younger than sedimentation of the Sodankylä Group quartzites and pelites, but it may be roughly coeval with the sedimentation of the Savukoski Group pelites, whose minimum age is given by overlying plume-related 2.06 Ga komatiites and basalts (Hanski et al., 2001b) and crosscutting 2.05 Ga intrusives (Mutanen & Huhma, 2001). These events may be related with mafic underplating and melting of the lower crust and coeval extension and thinning, causing deepening and subsidence of the basin in which the Savukoski Group sediments were deposited.

According to our data and previously published age determinations, the Central Lapland area was strongly affected by orogenic events throughout the period 1.85 – 1.76 Ga, producing large volumes of granitoids. Orogenic magmatism was also prominent during the interval 1.85 – 1.80 Ga in the southern and southwestern Svecofennian part of the Fennoscandian Shield, with abundant plutonic and volcanic rocks and intensive migmatisation (Korsman et al., 1984; Mansfeld, 1996; Åhäll & Larson, 2000; Andersson et al., 2001; Skridlaite & Motuza, 2001; Väisänen et al., 2002; Kurhila et al., 2005). In the central and northern parts of the Svecofennian domain, rocks of this age are less abundant, but the Molkokönġäs granite and the Pernu monzogranite represent this age group, as well as some granitoids in northern Sweden (e.g. Skiöld, 1988). The Molkokönġäs granite has a strong SW-NE trending foliation, which represents the regional D2 or D3 deformation (cf. Hölttä et al., in press). Consequently, the ion probe U-Pb age on zircon, 1855 ± 13 Ma, constrains the maximum age for the deformation of this rock.

Majority of the granitoids in this study are dated at around 1.79 – 1.76 Ga. This age can also be seen in the disturbance of the U-Pb system in hydrothermally altered rocks (Mänttäri, 1995) and as widespread U-Pb ages on titanite, monazite and rutile in Central and Western Lapland (Hiltunen, 1982; Lauerma, 1982; Rastas et al., 2001; Corfu & Evins, 2002), and also in the Karelian-Belomorian junction zone, where the titanite ages of 1.78 – 1.75 Ga are dominant (Bibikova et al., 2001). The Kappera sample is from the Hetta Complex (Fig. 1), from an area for which reliable conventional zircon data were previously unavailable. The Kappera rock is a foliated migmatite with a flat-lying structural orientation and although the Kappera outcrop is situated only ca. 50 km from the present contact of the Lapland Granulite Belt, the high-grade metamorphism is ca. 150 Ma younger than the Lapland-Kola orogen. As in most of our dated granitoids, the majority of the zircons in the Kappera rock crystallised from the leucosome melt at around 1774 Ma. The age of the leucosome, as well as the abundance of the 1.79 – 1.76 deformed granitoids indicate that ductile deformation, metamorphism and melting were widespread in this time interval. A similar conclusion was reached by Corfu & Evins (2002) who argued that monazite and titanite ages from the Archaean Suomujärvi Complex

(Evins et al., 2002), in the eastern part of the Central Lapland Granitoid Complex (Fig. 9) indicate that the major episode of deformation and metamorphism and associated granitic magmatism occurred in the period between 1780 and 1770 Ma and that metamorphic conditions persisted until about 1765 Ma. However, there are regional variations in the age of metamorphism as a consequence of various tectonic and magmatic events. According to Hölttä et al. (in press) the metamorphic grade increases from andalusite to sillimanite grade towards the contact of the Nilipää intrusion, and if this is related to the thermal effects of pluton emplacement, metamorphism in the Nilipää must also be of. 2.1 Ga age. Some zircons and zircon rims in our samples are relatively young, around 1.74 – 1.72 Ga. Because the 1.76 – 1.84 Ga intrusions dated in this study are mostly deformed, it is possible that young zircons record metamorphism and deformation, which can be at least locally as young as 1.74 – 1.72 Ga.

Some of the 1.80 – 1.77 Ga granites in northern Finland are highly discordant across their host rocks and have therefore been classified as postorogenic by e.g. Haapala et al. (1987), Front et al. (1989) and Nironen (2005). Our data show that this term cannot be used for most granitoids of this age in Lapland. Eklund et al. (1998) used the term post-collisional for Svecofennian intrusions of 1.8 Ga that occur in a 600-km-long belt in southern Finland and Russian Karelia from the Åland Islands to the NW Lake Ladoga region. These rocks range from ultramafic, calc-alkaline, apatite-rich potassium lamprophyres to peraluminous high Ba and Sr granites, forming a shoshonitic series. Andersson et al. (2006) argued that this shoshonitic magmatism could have been generated as a consequence of subduction beneath the continental margin in the southwest. The subduction was potentially associated with the Transscandinavian Igneous Belt (TIB) magmatism, which emplaced within the western margin of the Svecofennian domain at 1.85 – 1.65 Ga (e.g. Gorbatchev, 2004). The Jääskö appinitic monzonite, as well the other appinites in Lapland (Mutanen, 2003) resemble compositionally the shoshonitic rocks in the southern Svecofennian domain, interpreted to originate from enriched lithospheric mantle (Eklund et al., 1998; Väisänen et al., 2000; Andersson et al., 2006). Väisänen et al. (2000) argued that these shoshonitic magmas increased temperature in mid-crustal levels causing crustal anatexis and production of granitic melts. In the Central Lapland Granitoid Complex area the process may have been similar. The area shows strongly positive Bouguer anomaly, despite the abundance of low-density granitoids at the surface (Ruotoistenmäki, 1977; Koljonen, 1992; Mutanen, 2003). This suggests that below the granites there are large volumes of mafic rocks, which may represent underplating of mantle-derived mafic magmas that are cogenetic with the appinites and caused anatexis in their crustal country rocks. Whether such underplating in Lapland could have been related to the orogenic processes that produced the TIB is a challenging subject for future studies.

Acknowledgements

Tuula Hokkanen and Arto Pulkkinen are thanked for assisting in the isotope laboratory of the Geological Survey of Finland. Martin Whitehouse, Kerstin Lindén and Lev Ilyinsky are thanked for the help with the ion microprobe in the NORDSIM laboratory. Especial thanks to Irmeli Mänttäri in the GSF for the help with the analyses and interpretation of the data. Thorough reviews by Eero Hanski and Laura Lauri improved the manuscript considerably. The idea for researching the Suomujärvi Complex and its surroundings was provided by Kauko Laajoki from the University of Oulu. Tom Andersen and the personnel of the Geological-Mineralogical Museum of Oslo University are thanked for performing the facilities and assistance for sample processing and Sm-Nd analyses. Peter Sorjonen-Ward kindly corrected the English. This paper is NORDSIM publication number 180. The Nordsim facility is operated under an agreement between the research councils of Denmark, Norway, and Sweden, the Geological Survey of Finland, and the Swedish Museum of Natural History.

References

Åhäll, K.-I. & Larson, S.Å., 2000. Growth-related 1.85-1.55 Ga magmatism in the Baltic Shield; a review addressing the tectonic characteristics of Svecofennian, TIB 1-related, and Gothian events. Geologiska Föreningens i Stockholm Förhandlingar 122, 193–206.

Airo, M.-L. & Ahtonen, N., 1999. Three different types of Svecokarelian granitoids in southeastern Lapland: magnetic properties correlated with mineralogy. In: Autio, S. (ed.) Geological Survey of Finland, Current Research 1997-1998. Geological Survey of Finland, Special Paper 27, 129–140.

Andersson, U.B., 1991. Granitoid episodes and mafic-felsic magma interaction in the Svecofennian of the Fennoscandian Shield, with main emphasis on the ~1.8 Ga plutonics. Precambrian Research 51, 127–149.

Andersson, U.B., Wikström, A., Åhäll, K.-I. & Larson, S.Å., 2001. Growth-related 1.85-1.55 Ga magmatism in the Baltic Shield; a review addressing the tectonic characteristics of Svecofennian, TIB 1-related and Gothian events; discussion and reply. Geologiska Föreningens i Stockholm Förhandlingar 123, 55–61.

Andersson, U.B., Eklund, O., Fröjdö, S. & Konopelko, D., 2006. 1.8 Ga magmatism in the Fennoscandian Shield; lateral variations in subcontinental mantle enrichment. Lithos 86, 1-2, 110–136.

Berthelsen, A. & Marker, M. 1986. Tectonics of the Kola collision suture and adjacent Archaean and Early Proterozoic terrains in the northeastern region of the Baltic Shield. Tectonophysics 126, 31–55.

Bibikova, E., Skiöld, T., Bogdanova, S., Gorbatschev, R. & Slabunov, A., 2001. Titanite-rutile thermochronometry across the boundary between the Archaean Craton in Karelia and the Belomorian Mobile Belt, eastern Baltic Shield. Precambrian Research 105, 315–330.

Corfu, F. & Evins, P.M., 2002. Late Palaeoproterozoic monazite and titanite U–Pb ages in the Archaean Suomujärvi Complex, N-Finland. Precambrian Research 116, 171–181.

Daly, J.S., Balagansky, V. V., Timmerman, M.J., Whitehouse, M. J., de Jong, K., Guise, P. , Bogdanova, S., Gorbatschev, R. & Bridgwater D., 2001. Ion microprobe U-Pb zircon geochronology and isotopic evidence for a trans-crustal suture in the Lapland–Kola Orogen, northern Fennoscandian Shield. Precambrian Research 105, 289–314.

De La Roche, H., Leterrier, J., Grandclaude, P. & Marchal, M. 1980. A classification of volcanic and plutonic rocks using R1R2- diagram and major element analyses - its relationships with current nomenclature. Chemical Geology 29, 183–210.

DePaolo, D.J., 1981. Neodymium isotopes in the Colorado Front Range and crust-mantle evolution in the Proterozoic. Nature 291, 684–687.

Eklund, O., Konopelko, D., Rutanen, H., Fröjdö, S. & Shebanov, A.D., 1998. 1.8 Ga Svecofennian post-collisional shoshonitic magmatism in the Fennoscandian shield, Lithos 45, 87–108.

Evins, P.M. & Laajoki, K., 2002. Early Proterozoic nappe formation : an example from Sodankylä, Finland, northern Baltic Shield. Geological Magazine 139, 73–87.

Evins P.M., Mansfeld J. & Laajoki K. 2002. Geology and Geochronology of the Suomujarvi Complex: a new Archaean gneiss region in the NE Baltic Shield, Finland. Precambrian Research 116, 285–306.

Front, K. & Nurmi, P., 1987. Characteristics and geological setting of synkinematic Svecokarelian granitoids in southern Finland. Precambrian Research 35, 207–224.

Gorbatchev, R., 2004. The Transscandinavian Igneous Belt–introduction and background. In: Högdahl, K., Andersson, U.B. & Eklund, O. (eds.) The Transscandinavian Igneous Belt in Sweden; A review of its character and evolution. Geological Survey of Finland, Special Paper 37, 9–15.

Haapala, I., Front, K., Rantala, E. & Vaarma, M., 1987. Petrology of Nattanen-type granite complexes, northern Finland. Precambrian Research 35, 225–240.

Hanski, E.S., 1997. The Nuttio Serpentinite Belt, Central Lapland: an example of Paleoproterozoic ophiolitic mantle rocks in Finland. Ofioliti 22, 35–46.

Hanski, E., Mänttäri, I., Huhma, H. & Rastas, P. 2000. Post-1.88 Ga deposition of the Kumpu and Lainio group molasse-type sediments in northern Finland: evidence from conventional and NORDSIM zircon dating. In: Eide, E. (ed.) 24. Nordiske Geologiske Vintermøte, Trondheim 6.–9. Januar 2000. Geonytt (1), p. 75.

Hanski., E., 2001. History of stratigraphic research in northern Finland. Geological Survey of Finland. Special Paper 33, 15–43.

Hanski, E., Huhma, H. & Vaasjoki, M., 2001a. Geochronology of northern Finland: a summary and discussion. In: Vaasjoki, M. (ed.) Radiometric age determinations from Finnish Lapland and their bearing on the timing of Precambrian volcano-sedimentary sequences. Geological Survey of Finland, Special Paper 33, 255–279.

Hanski, E., Huhma, H., Rastas P. & Kamenetsky V. S., 2001b. The Palaeoproterozoic Komatiite–Picrite Association of Finnish Lapland. Journal of Petrology 42, 855–876.

Hanski, E. & Huhma, H., 2005. Central Lapland greenstone belt. In: Lehtinen, M., Nurmi, P.A. & Rämö, O.T. (eds.) Precambrian Geology of Finland – Key to the Evolution of the Fennoscandian Shield. Elsevier B.V., Amsterdam, pp. 139–193.

Hiltunen, A., 1982. The Precambrian geology and skarn iron ores of the Rautuvaara area, northern Finland. Geological Survey of Finland, Bulletin 318, 133 p.

Hölttä, P., Väisänen, M., Väänänen, J. & Manninen, T., 2007. Paleoproterozoic metamorphism and deformation in Central Lapland, Finland. Geological Survey of Finland, Special Paper 44, 9–58.

Huhma, H., 1986. Sm-Nd, U-Pb and Pb-Pb isotopic evidence for the origin of the Early Proterozoic Svecokarelian crust in Finland. Geological Survey of Finland, Bulletin 337. 48 p.

Koljonen, T. (ed.) 1992. Suomen geokemian atlas. Osa 2: Moreeni. The Geochemical Atlas of Finland, Part 2: Till. Geological Survey of Finland, Espoo, 218 p. + 9 app. maps.

Korsman, K., Hölttä, P., Hautala, T. & Wasenius, P., 1984. Metamorphism as an indicator of evolution and structure of the crust in Eastern Finland. Geological Survey of Finland, Bulletin 328, 40 p.

Krill, A.G., 1985. Svecokarelian thrusting with thermal inversion in the Karasjok-Levajok area of the Northern Baltic Shield. Norges Geologiske Undersøkelse Bulletin 403, 89–101.

Kurhila, M., Vaasjoki, M., Mänttäri, I., Rämö, T. & Nironen, M., 2005. U-Pb ages and Nd isotope characteristics of the lateorogenic, migmatizing microcline granites in southwestern Finland. Bulletin of the Geological Society of Finland 77, 105–128.

Lahtinen, R., Korja, A. & Nironen, M., 2005. Paleoproterozoic tectonic evolution. In: Lehtinen, M., Nurmi, P.A. & Rämö, O.T. (eds.) Precambrian Geology of Finland – Key to the Evolution of the Fennoscandian Shield. Elsevier B.V., Amsterdam, pp. 481–531.

Larson, S.Å. & Berglund, J., 1992. A chronological subdivision of the Transscandinavian igneous belt - three magmatic episodes? Geologiska Föreningens i Stockholm Förhandlingar 114, 459–461.

Lauerma, R., 1982On the ages of some granitoid and schist complexes in northern Finland. Bulletin of the Geological Society of Finland 54, 85–100.

Ludwig, K.R., 1991. PbDat 1.21 for MS-DOS: A computer program for processing Pb-U-Th isotope data. Version 1.08. U.S. Geological Survey Open-File Report 88-542, 35p.

Ludwig, K.R., 2001. Users Manual for Isoplot/Ex rev. 2.49. Berkeley Geochronological Center Special Publication No. 1a, 55 p.

Mansfeld, J., 1996. Geological, geochemical and geochronological evidence for a new Paleoproterozoic terrane in southeastern Sweden. Precambrian Research 77, 91–103.

Mänttäri, I., 1995Lead isotope characteristics of epigenetic gold mineralisation in the Palaeoproterozoic Lapland greenstone belt, northern Finland. Geological Survey of Finland, Bulletin 381, 70 p.

Mutanen, T. 2003. Magmatismi ja malminmuodostus. Loppuraportti toiminnasta 1998-2001. Hanke 2104001. Geological Survey of Finland, Report M10.4/2003/1, 41 p. (in Finnish).

Mutanen, T & Väänänen, J. 2004. PGE-Au-Cu-Ni potential of postkinematic appinitic (1.79 Ga) intrusions in Finland. In: 17th Australian Geological Convention, Hobart 8-13th February 2004. Dynamic Earth: Past, Present, and Future, Abstracts, p. 104.

Nironen, M. & Mänttäri, I., 2003. Structural evolution of the Vuotso area, Finnish Lapland. Bulletin of the Geological Society of Finland 75, 93–101.

Nironen, M., 2005. Proterozoic orogenic granitoid rocks. In: Lehtinen, M., Nurmi, P.A. & Rämö, O.T. (eds.) Precambrian Geology of Finland – Key to the Evolution of the Fennoscandian Shield. Elsevier B.V., Amsterdam, pp. 445–479.

Öhlander, B. & Skiöld, T. 1994. Diversity of 1.8 Ga potassic granitoids along the edge of the Archaean craton in northern Scandinavia; a result of melt formation at various depths and from various sources. Lithos 33, 265–283.

Rastas, P., Huhma, H., Hanski, E., Lehtonen, M. I., Härkönen, I., Kortelainen, V., Mänttäri, I. & Paakkola, J. 2001. U-Pb isotopic studies on the Kittilä greenstone area, central Lapland, Finland. In: Vaasjoki, M. (ed.) Radiometric age determinations from Finnish Lapland and their bearing on the timing of Precambrian volcano-sedimentary sequences. Geological Survey of Finland, Special Paper 33, 95–141.

Räsänen, J. & Huhma, H., 2001. U-Pb datings in the Sodankylä schist area, central Finnish Lapland. In: Vaasjoki, M. (ed.) Radiometric age determinations from Finnish Lapland and their bearing on the timing of Precambrian volcano-sedimentary sequences. Geological Survey of Finland, Special Paper 33, 153–188.

Richard, P., Shimizu, N. & Allègre, C.J. 1976. $^{143}Nd/^{146}Nd$, a natural tracer: an application to oceanic basalts. Earth and Planetary Science Letters 31, 269–278.

Ruotoistenmäki, T. 1977. Tutkimus Keski-Lapin graniittialueen rakenteesta. M.Sc. Thesis, University of Technology, Helsinki, 61 p.

Skridlaite, G. & Motuza, G., 2001. Precambrian domains in Lithuania: evidence of terrane tectonics. Tectonophysics 339, 113–133.

Skiöld, T., 1988. Implications of new U-Pb zircon chronology to Early Proterozoic crustal accretion in Northern Sweden. Precambrian Research 38, 147–164.

Skiöld, T., Öhlander, B., Markkula, H., Widenfalk, L. & Claesson, L.-Å., 1993. Chronology of Proterozoic orogenic processes at the Archaean continental margin in northern Sweden. Precambrian Research 64, 225–238.

Stacey, J.S. & Kramers, J.D. 1975. Approximation of terrestrial lead isotope evolution by a two-stage model. Earth and Planetary Science Letters 26, 207–221.

Taylor, S.R. & McClennan, S.M., 1985. The Continental Crust: its Composition and Evolution. Blackwell, Oxford, 312 p.

Tuisku, P. & Huhma, H., 1998. Eclogite from the marginal zone of the Lapland granulite belt: evidence from the 1.90-1.88 Ga subduction zone. Geological Survey of Finland, Special Paper 26, p. 61.

Väänänen, J. & Lehtonen, M., 2001.U-Pb isotopic age determinations from the Kolari-Muonio area, western

Finnish Lapland. In: Vaasjoki, M. (ed.) Radiometric age determinations from Finnish Lapland and their bearing on the timing of Precambrian volcano-sedimentary sequences. Geological Survey of Finland, Special Paper 33, 85–93.

Väisänen, M., Mänttäri, I., Kriegsman, L.M. & Hölttä, P., 2000. Tectonic setting of post-collisional magmatism in the Palaeoproterozoic Svecofennian Orogen, SW Finland. Lithos 54, 63–81.

Väisänen, M., Mänttäri, I. & Hölttä, P., 2002. Svecofennian magmatic and metamorphic evolution in southwestern Finland as revealed by U-Pb zircon SIMS geochronology. Precambrian Research 116, 111–127.

Väänänen, J., 2004. Sieppijärvi and Pasmajärvi. Explanation to the Geological map of Finland 1:100 000, pre-Quaternary rocks, sheets 2624 and 2642, 55 p. + 1 app. + 2 app. maps (in Finnish with English summary).

Wasserburg, G.J., Jacobsen, S.B., DePaolo, D.J., McCulloch, M.T. & Wen, T., 1981. Precise determination on Sm/Nd ratios, Sm and Nd isotopic abundances in standard solutions. Geochimica et Cosmochimica Acta 45, 2311–2323.

Whitehouse, M.J., Claesson, S., Sunde, T. & Vestin, J., 1997. Ion microprobe U-Pb zircon geochronology and correlation of Archaean gneisses from the Lewisian complex of Gruinard Bay, northwestern Scotland. Geochimica et Cosmochimica Acta 61, 4429–4438.

Whitehouse, M.J., Kamber, B. & Moorbath, S., 1999. Age significance of U-Th-Pb zircon data from early Archaean rocks of west Greenland – a reassessment based on combined ion-microprobe and imaging studies. Chemical Geology 160, 201–224.

Wiedenbeck, M., Allé, P., Corfu, F., Griffin, W.L., Meier, M., Oberli, F., von Quadt, A., Roddick, J.C. & Spiegeln, W., 1995. Three natural zircon standards for U-Th-Pb, Lu-Hf, trace element and REE analysis. Geostandards Newsletter 19, 1–23.